Journal of Climate Change
ISSN 2395-7611 Volume 12 (2026) No. 2. pp. 250–280

https://doi.org/10.70917/jcc-2026-015
Article

Adaptive Injection Phasing and Methanol Blend Optimization for Low-Carbon Engine Performance: A Meta-Analysis and Machine-Learning Framework with CCS Integration

Luke Ajuka [1,*] and Christopher Enweremadu [1]

[1] University of South Africa, Department of Mechanical, Bioresources, and Biomedical Engineering, Gauteng, Johannesburg, 1710, South Africa 1; ajukalo@unisa.ac.za(L.A)
* Correspondence author: ajukalo@unisa.ac.za; enwercc@unisa.ac.za

Abstract: The transition to net-zero mobility, aligned with global decarbonization targets, has intensified interest in methanol as a clean combustion fuel and carbon-neutral energy carrier. When optimally blended, methanol's high-octane rating, strong charge-cooling effect, and inherent oxygen content enhance brake thermal efficiency (BTE), improve premixed combustion, and suppress knock in both spark- and compression-ignition engines. This study integrates meta-analysis, physics-informed modelling, and machine learning to establish predictive relationships between methanol blend ratio, start-of-injection (SOI) phasing, and engine performance. Meta-analysis revealed a significant positive correlation between SOI advancement and BTE ($r = 0.74$, 95% CI: 0.60–0.85), with moderate heterogeneity ($I^2 = 38–45\%$). Optimal performance was achieved at methanol blend ratios of 25–30% with SOI between −30° and −35° CA aTDC, balancing efficiency gains with emission constraints. Quantitative model evaluation demonstrated high predictive accuracy ($R^2 \approx 0.99$, RMSE < 0.30), exceeding typical machine learning combustion models ($R^2 \approx 0.91–0.97$). SHAP-based sensitivity analysis confirmed that methanol blend ratio (0.125 ± 0.015) and SOI (0.082 ± 0.010) are dominant parameters controlling system behaviour. Model comparison showed that XGBoost achieved the highest accuracy (MAE = 0.01 °CA, RMSE = 0.02 °CA, $R^2 = 0.985$), outperforming Random Forest ($R^2 = 0.90$) and the physics-informed correlation model ($R^2 = 0.93$), while linear regression exhibited inferior performance ($R^2 = 0.90$) due to its inability to capture nonlinear interactions. Residual analysis (±0.4 BTE) and validation with 95% confidence bands (±0.42 BTE) confirmed strong predictive reliability and generalisation. The integration of carbon capture and utilization (CCU) pathways with methanol synthesis further supports closed-loop CO_2 utilisation, reinforcing methanol's potential in carbon-neutral and carbon-negative applications. Overall, the findings highlight the importance of adaptive, AI-driven SOI optimisation and integrated CCU strategies for advancing next-generation low-emission engine systems.

Keywords: Decarbonization; Carbon capture and storage; Physics informed machine learning; Combustion ignition engines; SOI optimization; Sensitivity analysis

Nomenclature

TSA	-	Temperature swing adsorption
CCU	-	Carbon capture and utilization
IRR	-	Internal Rate of Return
SCR	-	Selective catalytic reduction
aTDC	-	After top dead center
PtMeOH	-	Power-to-Methanol
DPF	-	Diesel particulate filters
GTL	-	Gas-to-Liquid
SOI	-	Start of Injection
NOx	-	Nitrogen oxides (NO, NO_2)

PFI	-	Port Fuel Injection	Da	-	Damköhler number
WIT	-	Water injection timing	WFR	-	Water-fuel ratio
IMEP	-	Indicated mean effective pressure	EOI	-	End of injection timing
IRGR	-	In- cylinder reforming gas recirculation	ECE	-	Energy conversion efficiency
PPCI	-	Partially premixed compression ignition	TRLs	-	Technology readiness levels
GSDR	-	Gas Switching Dry Reforming	EGR	-	Exhaust gas recirculation
R^2	-	Coefficient of determination	CI	-	Confidence interval
MAE	-	Mean absolute error	RF	-	Random Forest
CES	-	Combined effect size (meta-analysis)	SHAP	-	SHapley Additive exPlanations.

Graphical Abstract

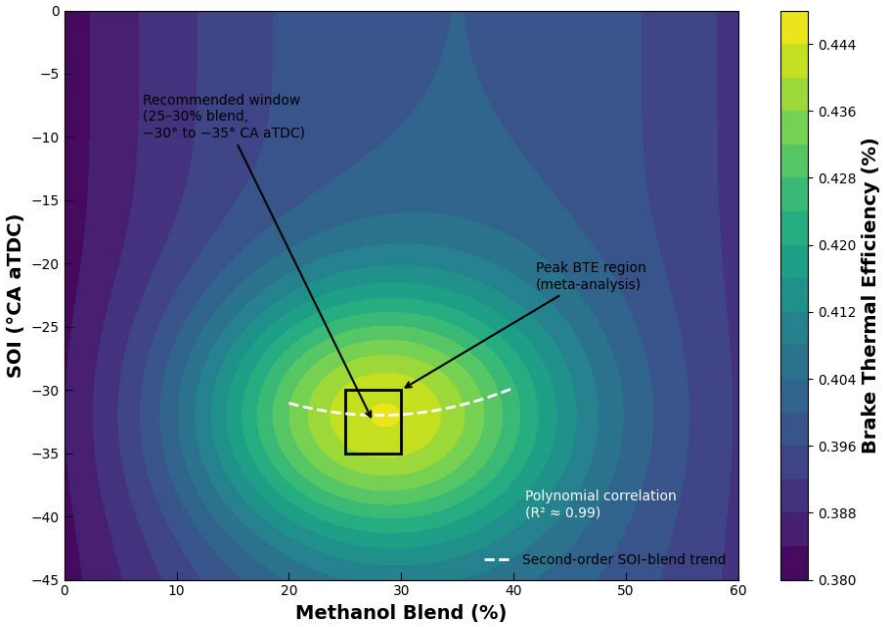

1. Introduction

In response to energy security concerns and escalating climate change, the majority of which have been generated by human activities since the pre-industrial era (Razak *et al.*, 2025; Riffat *et al.*, 2026), there is an urgent need for clean and sustainable energy carriers capable of accelerating global decarbonization. Fossil fuel burning remains the principal source of anthropogenic greenhouse gas emissions, mainly CO_2 (Bakhsh and Cantino, 2025; Shen and Yang, 2026). This highlights the need for a shift towards carbon-neutral or even carbon-negative energy sources. Methanol's liquid form makes it an enticing option among renewable alternatives, including CO_2 hydrogenation and renewable energy (Olah *et al.*, 2018; Bos *et al.,* 2020).

Methanol has several advantages over conventional fuels (Table 1). Experimental studies have shown that even minimal methanol mixing with other fuels can improve engine combustion performance by boosting efficiency at lower temperatures while lowering hydrocarbon (HC) and carbon monoxide (CO) emissions (Berber, 2019; Duan *et al.*, 2023). These findings are supported by studies on a wide range of engine applications, including spark ignition engines (SIE) (Duan *et al.*, 2023), compression ignition engines (CIE) (Karvounis *et al.*, 2023), internal combustion engines (Zhen and Wang, 2015), and gas turbines (Wu *et al.*, 2024).

The Intergovernmental Panel on Climate Change (IPCC) highlights the importance of limiting global warming to 1.5°C through policies such as reducing energy intensity, accelerating decarbonization, and developing carbon capture technologies (Vitillo *et al.*, 2022), and this call to action emphasizes renewable energy as a key component of climate mitigation. Carbon capture and utilization (CCU) decrease CO_2 emissions and turns them into useful fuels like methanol. Meanwhile, carbon capture and methanol synthesis can simultaneously solve global warming and energy demand concerns, as well as long-term environmental goals (Scripps, 2025), especially when supported through machine learning optimization (Samavedam et al., 2026; Ajuka and Enweremadu, 2026).

Table 1. Multi-criteria comparison of methanol with selected alternative fuels for engine application, storage, compatibility, environmental performance, and market readiness (IEA, 2021; Xing *et al.*, 2021).

Criteria	Methanol	Ethanol	Biodiesel	Hydrogen	Ammonia	Natural Gas (CNG/ LNG)
Source Versatility	Can be made from CO2 + H2, biomass, municipal waste, or electricity (power-to-methanol)	Biomass-based only	Vegetable oil/fatty acid feedstock	Water electrolysis or natural gas reforming	Electrolysis or fossil ammonia routes	Fossil (but also biogas origin possible)
Liquid at Ambient Conditions	Yes (easy storage, handling, and transport)	Yes	Yes	No (needs compression or liquefaction)	Yes, but toxic and corrosive	CNG is compressed; LNG requires cryogenics
Engine Compatibility	Works in spark-ignition (SI), dual-fuel CI, and modified CI engines	SI engines	CI engines (with limited blends)	Requires new engine platforms	Requires special ignition systems	With minor modifications
Combustion Cleanliness	Low soot, high flame speed, no sulfur	Moderate soot	More soot and NOx	Zero carbon, but NOx possible	Zero carbon, but high NOx	Moderate CO2 and methane slip
Octane Number / Knock Resistance	Very high (RON approximately110), excellent anti-knock properties	High (RON approximately108)	Low	N/A (not used in SI engines)	N/A	Moderate
CO_2 Neutrality Potential	High (when made from renewable CO2 and H2)	Medium (depends on agricultural input)	Medium	Zero-carbon if green hydrogen	Carbon-free (but lifecycle dependent)	Fossil-based mostly
Infrastructure Compatibility	Can use existing pipelines and tanks with minor modifications	Similar	Similar	Needs dedicated pipelines and tanks	Needs corrosion-resistant infrastructure	High-pressure tanks and compressors
Toxicity & Safety	Toxic if ingested/inhaled; flammable	Lower toxicity	Low toxicity	Explosive and leak-prone	Toxic, pungent, and corrosive	Risk of methane leaks (GHG potential)
Production Energy Cost	Moderate, decreasing with green H_2 scale-up	Low to moderate	Moderate	High (if green)	High (electrolysis-based routes)	Moderate to low
Market Readiness / Maturity	Moderate – growth in marine, industrial, and road fuel applications	High	High	Low (nascent)	Low to moderate	High

Table 1 shows that methanol may be produced from captured CO_2 and renewable hydrogen, consequently promoting circular carbon cycles and negative-emission pathways when combined with renewable energy systems (Xing *et al.*, 2021). Unlike gaseous options such as hydrogen or ammonia, methanol is a liquid at ambient temperatures and is compatible with present engine topologies, requiring only minor modifications for deployment. Its favorable combustion features, such as low soot emission, high laminar flame speed, and latent heat of vaporization, enhance charge cooling and allow for cleaner, more efficient combustion than diesel or biodiesel (Yao and Yao, 2023). Methanol is easier to handle, store, and transport than hydrogen or natural gas because it does not require high-pressure tanks or cryogenic infrastructure (Duan *et al.*, 2023). When produced from renewable sources, it is carbon-neutral; however, future integration with onboard or exhaust-based carbon capture technologies may allow for carbon-negative operation (Wu *et al.*, 2024).

Methanol (CH_3OH) has been used as an engine fuel since the early 1900s. It was first employed in aviation and motorsports due to its high-octane rating and clean combustion. During the 1930s, European Grand Prix racing used methanol-based mixes (usually M86 mixed with acetone, nitrobenzene, and ether) to boost combustion performance (Germane, 1985). Later, in the United States and China, methanol and its blends were examined for use in flexible-fuel vehicles to diversify fuel supply and minimize petroleum dependence (Yao and Yao, 2023; Bromberg and Cheng, 2021). Beyond transportation, methanol has long been utilized in model aircraft engines, racing applications, and tractor pullers due to its high ignition temperature, super-octane equivalent, anti-freeze capacity, and ability to suppress engine

deposits (Bromberg and Cheng, 2021). Meanwhile, methanol fires are also more manageable than petroleum fires, being extinguishable with water.

Recently, interest has shifted to renewable methanol (green methanol), manufactured from collected CO_2 and hydrogen supplied by renewable energy. A balance of combustion emissions with captured CO_2 during synthesis is an approach that can provide a closed carbon loop and considerably reduce net greenhouse gas emissions. In another ecofriendly form, renewable methanol is equally appropriate for SI and dual-fuel CI engines because of its low soot generation, high oxygen content, and great knock resistance. Figure 1 displays current research trends, highlighting the growing importance of renewable methanol in decarbonizing energy-intensive sectors.

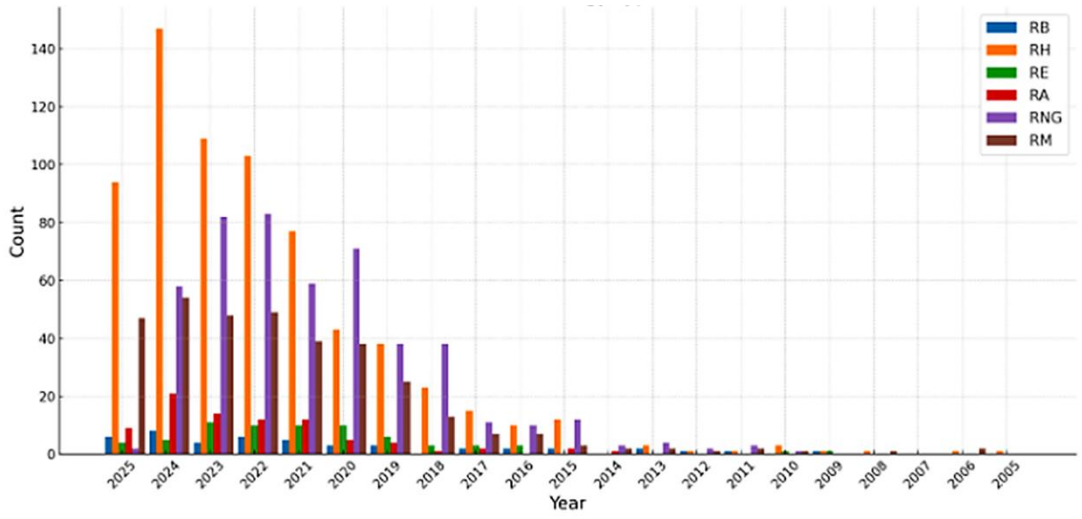

Figure 1. Trend in Renewable Fuel Types (2005-2025) [Sciencedirect.com]. Note: RH - Renewable hydrogen, RNG - renewable natural Gas, RM - renewable methanol, RE - renewable ethanol, RA - renewable ammonia, RB - renewable biodiesel.

Figure 1 supplemented the annual releases on various renewable fuel types, and observation shows that renewable hydrogen and methanol have consistently dominated in recent years, indicating robust research and deployment, which may be linked to the decarbonization of heavy industries and transport. RH and RM are on a more stable upward trend, showing mature technology and acceptance. RNG has shown unpredictability in recent years, peaking in 2023-2024, possibly because of waste-to-energy projects and methane capture incentives. Meanwhile, RE and RA continually increase with moderation, with RE peaking after 2023, RA's application increased after 2021, and RB's low count in comparison to others implies market saturation or replacement by other fuels.

Other comparative benefits of RM include the renewable methanol's (RM) clean energy transition potential. It is extremely versatile, serving as a direct transportation fuel, a gasoline blend component, an IMO sulfur-compliant marine fuel, and a feedstock for olefins, formaldehyde, and other chemicals. Unlike renewable hydrogen, RM allows for simple storage, transit, and use in existing fuel infrastructure without modification. Its production from CO_2 and green hydrogen promotes carbon recycling and supports carbon-neutral or even carbon-negative pathways, particularly when biogenic CO_2 sources are used. RM production is more energy-efficient and cost-effective than hydrogen generation as it utilizes current industrial processes like biomass, municipal waste, or CO_2-H_2 synthesis. Increased popularity in the maritime sector demonstrates RM's regulatory compliance and practical scalability, while its lower toxicity and explosion risk compared to hydrogen and ammonia enhances safety during handling and operation (Methanol Institute, 2018).

1.1. Knock, Miscibility and Injection

Methanol has excellent knock-resistant characteristics, which makes it ideal for use in internal combustion engines (Yao and Yao, 2023). Its high-octane rating (RON 52-57, MON 31-34) and improved knock resistance enable higher compression ratios than gasoline (RON 33-40) without detonation, thereby increasing thermal efficiency. Its high latent heat of vaporization (1100 kJ/kg, close to four times that of gasoline) provides a strong charge-cooling effect, lowering intake mixture temperatures by 20–30 °C, reducing peak in-cylinder temperatures, and suppressing knock. With an approximate of 50% oxygen by mass, methanol promotes more complete combustion, minimizes carbon

deposits, and reduces hot-spot-induced knock. Experimental studies show that methanol–gasoline blends (M15–M85) extend knock-limited spark advance by 3–8 crank-angle degrees in spark-ignition engines, while suppressing knock under high-load dual-fuel diesel–methanol conditions, enabling downsizing and turbocharging without compromising durability (Schröder *et al.*, 2020). From a combustion theory perspective, knock suppression involves shortening normal flame propagation time to the end-gas (t_1) while extending the time before end-gas auto-ignition (t_2) (Kalwar *et al.*, 2023). Although knocks are linked to auto-ignition, not all auto-ignitions induce knock (Netzer *et al.*, 2019), as shown in Figure 2. Auto-ignition modes can be classified by temperature gradient into laminar flame propagation, deflagration, detonation, or thermal explosion (Bradley *et al.*, 2022). The Damkohler effect estimated through the Damkohler number (Da) defines the ratio of chemical reaction time to transport time (equation 1), where molecular viscosity (ν) and laminar flame speed (S_l) are key parameters, with coefficient f_c typically assumed unity (Keum and Kuo, 2019). When Da $\gg$ 1, reactions proceed faster than transport, and allow mixture to reach ignition temperature rapidly, increasing auto-ignition probability further explains ignition through the ratio of diffusion to reaction timescales (Hayashi *et al.*, 2022).

$$D_a = \frac{\tau_D}{\tau_c} \tag{1}$$

where; $\tau_D = \frac{\nu}{S_L^2}$, and $\tau_D = f_c \times \tau_{ig}$.

Conversely, Da $\ll$ 1 indicates transport dominance, slowing ignition and reducing auto-ignition likelihood. Da is widely applied in combustion research, including flameless combustion design (Rasaq *et al.*, 2025), reactor sizing and scale-up (Otalvaro Marín and Machuca Martínez, 2020), residence time–kinetics trade-offs in methanol steam reforming (Wijaya *et al.*, 2012), and soot reduction studies in non-premixed flames (Attili *et al.*, 2015). The relevance of Da is further demonstrated by its methanol-specific behaviour. According to Wang *et al.* (2023), there is a negative temperature coefficient (NTC) behaviour under fuel-rich circumstances at elevated pressures, where rising Da increase's reaction dominance and decreases reaction rates with temperature. Similarly, Stauch and Maas (2008) demonstrated that increasing ambient temperature elevates Da, accelerating chemical kinetics and making transport more rate-limiting, hence influencing ignition delay.

These behaviours are closely linked to knock reduction approaches such as delayed ignition time (DIT), fuel enrichment, and the use of high-octane fuels (Zhen *et al.*, 2012). Methanol's soot-free combustion and octane properties are beneficial, but its downsides include low energy density, poor diesel miscibility, corrosivity, and poor lubrication (Paltrinieri *et al.*, 2019). Methanol's gasoline-like properties (Bromberg and Cheng, 2010) and renewable production paths, such as CO_2 hydrogenation with green hydrogen (Wang *et al.* 2026), support its position in the sustainable energy transition.

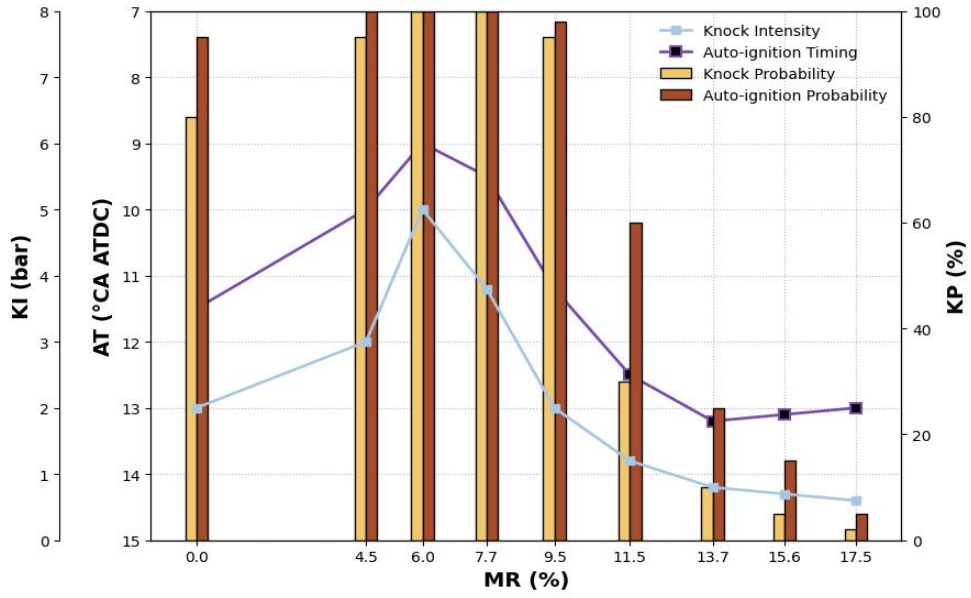

Figure 2. Variation of knock intensity (KI), auto-ignition timing (AT), knock probability (KP), and auto-ignition probability as a function of methanol ratio (MR). Line plots represent knock intensity and auto-ignition timing. Adapted from (Zhou *et al.*, 2022).

The figure illustrates the combined influence of methanol addition on knock behaviour and combustion phasing under the different operating conditions. The rising influence of methanol percentage on ignition delay and knock behaviour at low blend levels (0-4.5%) demonstrates that knock intensity begins slowly but rapidly grows, while auto-ignition probability which exceeds 70%, indicates high reactivity and unstable combustion (Figure 3). At moderate fractions (6-7.7%), the most severe knock conditions occur, with severity peaking at 6 bar and likelihood remaining around 80%. Knock becomes more noticeable as auto-ignition approaches TDC, indicating a critical blending window where methanol destabilizes combustion, and higher ratios (≥11.5%) lead to lower knock intensity, likelihood, and auto-ignition. This shift focuses on methanol's cooling and evaporation effects, which stabilize combustion and delay ignition timing at ATDC, implying a safer operating regime. Whether neat or blended, Methanol is entirely miscible with water, causing flame extinction during droplet burning and deviating from the normal d^2-law. Low Damkohler numbers limit chemical heat release in the liquid sphere, causing extinction at crucial droplet sizes (Yu *et al.*, 2024; Rehage and Kind, 2020). Higher-carbon isomers are recommended to reduce phase instability in gasoline-methanol combinations (*Xu et al.*, 2023). Impurities such as ethanol or halide ions improve electrical conductivity, increasing the danger of electrochemical and galvanic corrosion in simple methanol (Figure 3), while a mixture of gasoline-methanol-ethanol have poor conductivity (approximately 10 µS/m) (Geng *et al.*, 2025).

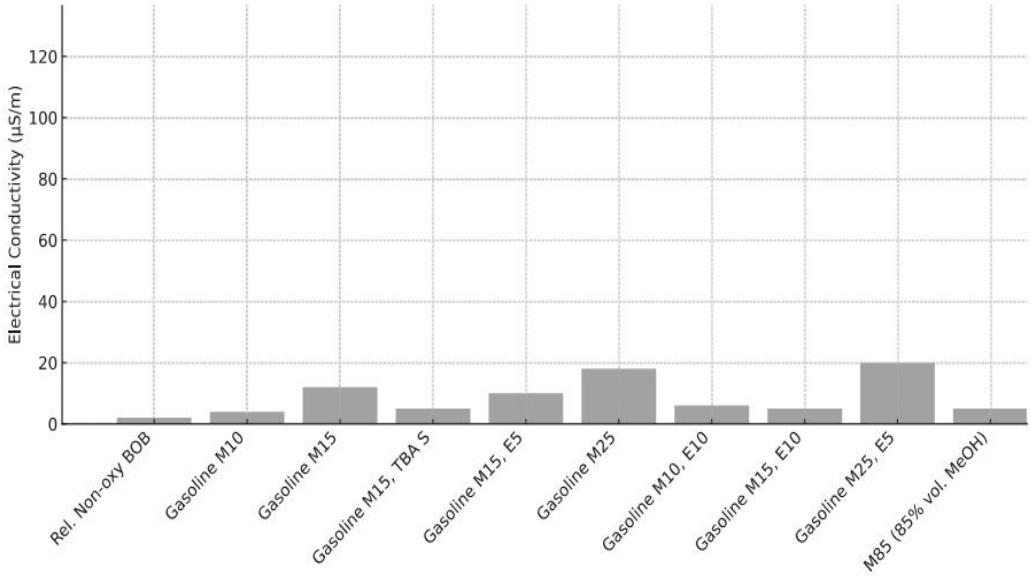

Figure 3. Electrical conductivity values gasoline + EtoH + MeoH. Adapted from Li *et al.* (2022).

Methanol fuel standards vary globally. In Europe, the Fuel Quality Directive (2009/30/EC) and EN 228 allow up to 3 vol.% methanol in gasoline. In the U.S., ASTM D4814-10a permits 0.3–2.75 vol.% with butanol or higher alcohols, while the EPA 'Octamix waiver' allows 2.5–5 vol.% co-solvents. China's national standard authorizes allows for 85% (M85), with provincial regulations allowing 5–100% blends, reflecting diverse regulatory and infrastructural contexts (Methanol Institute, 2020).

1.2. Optimal Injection Ratio for Knock Suppression

Methanol acts efficiently as anti-knock agent in gasoline engines, owing to its high latent heat of vaporization, which reduces the tendency to knock and lowers combustion temperature (Yates *et al.*, 2010). Methanol's charge-cooling action, chemical influence, and octane sensitivity all work together to minimize knock, with cooling being particularly effective in both plain methanol and blended fuels (Wang *et al.*, 2019). Liu *et al.* (2024) found that direct water injection in high-compression-ratio engines improved knock suppression and droplet dispersion. The ideal timing (−80 °CA) reduced mixture temperatures below 760 K. At ignition timings of 2°CA and −3°CA, thresholds for water-fuel ratios (0.4 and 0.6) were identified, with knock severity decreasing as WFR increased. Nonetheless, challenges persist, particularly in mixture formation, as noted by Wei *et al.* (2023) and highlighted in Table 2.

Table 2. Methanol Injection-Emission Studies on Engines

Work done	Mechanism/Process	Remark/Outcome	Reference
The influence of injecting methanol into a gasoline engine under heavy load conditions (1500 rpm, 120 kPa) as an anti-knock agent using a modified low-flow direct injection within the cylinder highload turbo-charged port was investigated in this study.	The impact of methanol injection timing and methanol ratio on knock suppression was examined using early and late injection timings, auto-ignition timing, and knock intensity (KI) and knock probability to quantify the knock.	The report states that the timing of methanol injection has a significant impact on combustion and that injecting fuel near the BDC may result in the greatest knock reduction. Toward the end of the compression stroke, a low methanol ratio will make the knock phenomenon more intense. In the meantime, when methanol was supplied late in the compression stroke, neither high nor low methanol ratios significantly decreased the knock or increased its intensity.	Yu *et al.* (2024)
The impact of knock combustion and direct injection on knock suppression were examined in this study using a single-cylinder, naturally aspirated SI engine with a high compression ratio of 15.	The methanol engine's knocking characteristics with a stoichiometric mixture was assessed under port fuel injection mode. To minimize the knocking combustion, they used a methanol direct injection technique to maximize the charge cooling effect.	Knocking combustion was found to occur at medium and high loads, intensify at indicated mean effective pressure (IMEP) of 0.7 MPa, and produce random heavy knock cycles with ultra-high knock intensity at 2.5% frequency. The maximum oscillating pressure amplitude reached 2.39 MPa. They determined that pre-ignition from specific hot spots in the combustion chamber was the cause of the loud knock. To reduce the knock intensity by 14.3%, they recommended an ideal split injection rather than a single injection.	Duan *et al.* (2022)
A 0.55L single-cylinder engine with a compression ratio of 10.9:1 running at 800 kPa net IMEP and 1500 RPM was used to investigate how water-methanol injection affected the performance of gasoline direct injection engines.	With a baseline test that did not involve water injection, direct injection tests were carried out using gasoline fuel mixed with 10% ethanol (E10). Additionally, port injection was used with four different mixtures: 100% methanol, 50% water + 50% methanol, 75% water + 25% methanol, and 100% water.	Since the combustion phase is sensitive at advanced spark timings, they found that adding water and water-methanol blends improved the engine's combustion stability and reduced IMEP fluctuation. Furthermore, the combined effects of an improved combustion phase and increased charge cooling result in lower exhaust gas temperatures when water and water-methanol mixes are added.	Miganakallu *et al.* (2020)
Study examines the injection strategy on a heavy-duty SI-methanol engine's injection technique for knock suppression and thermal efficiency through cylinder-to-cylinder variation.	The impact of an intake stroke with high injection pressure was established using both simulation and experimentation, considering the relationship between intake flow and spray.	It was observed that the spray and intake flow strongly interact to create a more uniform and drop in the temperature mixture that lengthens the end-gas ignition delay. As opposed to the knock propensity, at injection timing (αinj) of 320ºCA to 480ºCA, the combustion speed and thermal efficiency first rise and subsequently fall. The homogenous mixture leads to higher thermal efficiency with a faster combustion speed record at αinj of 380ºCA, while the higher temperature of 480ºCA causes knock tendency, which shows a significant cylinder-to-cylinder variation in knock tendency with respect to in-cylinder temperature and pressure.	Zhu *et al.* (2022)
The impact of injection timing (αinj) on methanol's combustion, emissive properties, and mixture formation process was investigated.	A HD PFI SI engine running on pure methanol was used for simulations and experiments to study mixture formation at injection timing (αinj) temperatures of 240ºCA, 360ºCA, and 480◦CA. as well as up to 720◦CA in terms of emissions.	Premix and spray were the best mixture among the three mixture formations reported at the corresponding injection timing (αinj) temperatures: premix and spray, spray, and premix and spray. This was determined by homogeneity and lowering the in-cylinder mixture temperature. The leaner mixture near the spark plugs and the lower mixture lengthened or retarded CA0-10, CA10-90, and CA50, which resulted in a reduced engine brake thermal efficiency (BTE) at αinj of 120◦CA to 300◦CA due to the combustion characteristics. On the other hand, CO emissions decreased while HC emissions first increased and then decreased, whereas αinj varied between 0◦CA and 720◦CA. The CO and HC emissions were caused by the richer mixture volume in the combustion chamber region and the in-cylinder mixture temperature, respectively. The HC emission was caused by the richer mixture region in the fissure formed by the piston and liner.	Feng *et al.* (2024)
The study examined the effects of the methanol direct injection technique on the combustion and emission characteristics of a dual-fuel turbocharged engine running at a high load of 1500 rpm.	Five distinct methanol injection timings were investigated at various methanol energy substation ratios. These timings ranged from − 330◦ CA to − 60◦ CA ATDC. Among the attributes examined was the optimal injection and emissions.	The findings demonstrate that varying injection timings had distinct effects on engine combustion and emission parameters. The result of ending the injection timing of methanol (EOI) at 180◦ CA ATDC was the fuller atomization of methanol, which had the lowest knock intensity, the highest IMEP, the largest NOx emissions, and delayed combustion and decreased the combustion rate. They concluded that the optimal injection strategies were EOI = − 180◦ CA ATDC and an energy substation ratio range of 4.6% to 8.9%.	Shen *et al.* (2023)
This study examined the potential benefits of high CR and methanol direct injection (MDI) for enhancing engine performance using a 1.5-liter spark ignition passenger car engine and a miller cycle.	The engine was evaluated utilizing methanol and gasoline in stoichiometric combustion at BMEPs of 1.1 MPa and 1.5 MPa with CR11.5, CR13.8 and CR15.3. The performance cases of CR11.5 and CR15.3 with gasoline and methanol were compared under low burn combustion.	Fuel economy for gasoline decreases when CR is increased from 11.5 to 15.3 under stoichiometric combustion, but methanol exhibits the exact opposite trend. An elevated CR of 15.3 and MDI increased BTE to 43.3% at λ (excess air/fuel ratio) of 1.0, while a further application of lean burn increased BTE of methanol by 44.9% at CR15.3. This contrasts with 37.4% of gasoline at CR11.5. In the meantime, high CR and MDI prolonged combustion times for all designated λs, but because of their greater surface/volume ratio and flame dowsing, and at high λs, they released more CO and THC than low CR with gasoline.	Lee *et al.* (2020)

Table 2 shows that methanol injection strategy strongly governs combustion phasing, knock suppression, and emission formation. Across the reviewed studies, advanced or optimized SOI generally improves premixing and thermal efficiency, whereas delayed injection tends to reduce NO_x at the expense of increased CO/HC and lower combustion efficiency. Water–methanol or split-injection strategies further enhance knock mitigation by strengthening charge cooling and improving combustion stability. Overall, the evidence confirms that injection timing remains a primary control variable in determining the efficiency–emission trade-off in methanol-fuelled engines.

Despite its benefits, methanol combustion still emits CO_2, and its lower heating value compared to traditional hydrocarbon fuels results in efficiency losses. Furthermore, because to its corrosive nature, specialist materials and lubrication procedures are required to maintain long-term engine durability (Xing *et al.*, 2021). These constraints highlight the need for enhanced injection tactics, effective after-treatment systems, and adaptable engine designs to fully realize methanol's potential as a sustainable fuel. Recent studies have increasingly focused on integrating carbon capture technology directly into mobile combustion systems. While they are widely established in stationary applications, their use in vehicles and distributed power generation is still in its early stages. New technologies, such in-cylinder adsorption, post-combustion exhaust separation, and CO_2 exhaust gas recycling, show promise for reducing emissions at the source (Yao and Yao, 2023; Lee *et al.*, 2020). Coupled with renewable methanol, such capture-enhanced systems could surpass carbon neutrality, enabling carbon-negative operation. However, technological obstacles arise during integration. Fuel spray atomization, penetration, and evaporation significantly impact combustion efficiency and CO_2 exhaust distribution, impacting capture feasibility (Zhou *et al.*, 2022). While ex-situ CO_2-to-methanol conversion has great selectivity, scaling in-cylinder procedures is hindered by catalyst stability under high-temperature, high-pressure conditions. Advances in computer modelling, catalyst creation, and hybrid integration offer exciting opportunities, but practical implementation remains elusive. This study assesses the technological maturity and feasibility of large-scale CO_2-methanol integration.

Although methanol combustion and CO_2 utilization have each been widely studied, their integration remains insufficiently quantified from the standpoint of injection control, combustion optimization, and predictive system-level modelling.

To address these gaps, the present study advances a unified hybrid modelling framework for methanol-fuelled combustion systems that explicitly integrates three components that are usually treated separately in previous existing studies: (i) quantitative meta-analysis of published start-of-injection (SOI), blend ratio, efficiency, and emission data; (ii) physics-informed surrogate modelling to preserve mechanistic consistency between combustion phasing and engine response; and (iii) machine-learning-based prediction and optimization of brake thermal efficiency (BTE) under emission constraints. The novelty of this work lies not only in combining these methodological layers within a single computational pipeline, but also in using the meta-analytic evidence as statistical priors and the physics-based relationship as a governing constraint for model training. This integrated framework improves interpretability, reduces purely empirical model dependence, and provides a scalable basis for predictive control of methanol combustion systems under practical injection–blend–emission trade-offs. Therefore, the main contributions of this study are threefold: (1) to synthesize methanol combustion evidence into a harmonized quantitative database focused on SOI, blend ratio, BTE, and emissions; (2) to develop a physics-informed predictive framework that constrains machine learning with combustion-relevant relationships; and (3) to identify the coupled influence of SOI and methanol blend ratio on efficiency–emission trade-offs through validated optimization.

2. Methanol Potential Pathways

Most methanol produced globally is still made from fossil fuels, primarily synthesis gas, which is made from coal or natural gas and is made up of carbon dioxide (CO_2), hydrogen (H_2), and carbon monoxide (CO). GHG emissions during the lifecycle are largely caused by these pathways. while methanol combustion continues to release CO_2. Additionally, its relatively low heating value and corrosive properties present challenges for durable, high-efficiency engine applications (Xing *et al.*, 2021). Renewable methanol, by contrast, can be synthesized through catalytic hydrogenation of captured CO_2 with renewable hydrogen, producing methanol and water (Eq. 2):

$$CO_2 + 3\ H_2 \rightarrow CH_3OH + H_2O \quad (2)$$

This sustainable approach mitigates environmental consequences and promotes low-carbon transitions. Municipal solid waste, agricultural wastes, forestry byproducts, and renewable hydrogen are all used as feedstock (Methanol Institute, 2019). Renewable methanol emits approximately 95% less CO_2 and 80% less NO_x than fossil fuels and eliminates SO_x and particulates (Deka *et al.*, 2022). Its integration with carbon capture and storage (CCS) via pre-, post-, or oxy-fuel processes enhances decarbonisation

(Lyons *et al.*, 2021). Figure 4 depicts the different synthesis paths, with ethanol-producing locations providing promising opportunities for renewable methanol, particularly when wind or nuclear energy is abundant (Cordero-Lanzac *et al.*, 2022). When renewable hydrogen generation efficiency is around 70%, energy conversion efficiency (ECE) increases to around 49% (Giuliano *et al.*, 2020).

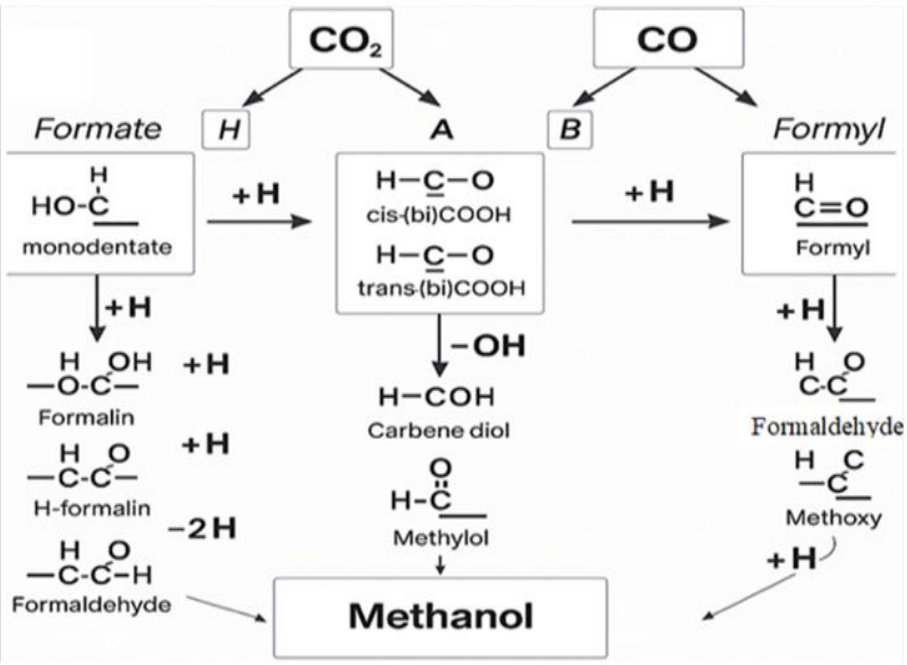

Figure 4. Typical Pathways for CO_2-to-Methanol Conversion. Adapted from (Chen *et al.*, 2019; Ren *et al.*, 2022).

The mechanistic interpretation of Figure 4 shows the principal pathways involved in CO_2 hydrogenation to methanol. Three dominant routes are recognized: the formate pathway, carboxyl pathway, and CO (carbon monoxide) pathway, each characterized by distinct intermediate species and reaction sequences. In the formate pathway, CO_2 is initially converted to formate species (monodentate or bidentate), which undergo sequential hydrogenation to formalin, formaldehyde, and ultimately methanol (Chen *et al.*, 2019; Ren *et al.*, 2022). The carboxyl pathway proceeds through the formation of cis- or trans-bidentate carboxyl intermediates, followed by hydrogenation to carbene diol and subsequent dehydration to yield methanol directly (Liang *et al.*, 2023). Alternatively, the CO pathway operates via two sub-branches: direct hydrogenation of CO to carbene diol and methanol (Zhu *et al.*, 2020), or through a formyl route, wherein successive hydrogenations transform CO to formyl (–CHO), formaldehyde, and methoxy (–OCH_3) intermediates before culminating in methanol (Higham *et al.*, 2025). Collectively, these pathways involve stepwise hydrogenation, dehydration, and rearrangement reactions that converge toward methanol as the ultimate product, highlighting the mechanistic versatility of CO_2 reduction chemistry.

2.1. Renewable Methanol, Storage and Carbon Capture Potential

The CO_2 capture and storage process begins with exhaust in ICEs, which are the main source of emissions. A waste heat recovery (WHR) system extracts thermal energy from hot exhaust gases, which can then be reused in downstream processes and improve overall system efficiency. Dehumidification removes moisture and preserves sorbent materials from deterioration, ensuring effective CO_2 capture optimal performance, and after drying, the exhaust stream is selectively separated using solid sorbents or structured adsorbent beds, resulting in a concentrated CO_2 stream.

Captured CO_2 is compressed and stored in high-pressure tanks for transportation and downstream use in processes including EOR, carbonation, and permanent geological sequestration. This sequential approach ensures that waste energy recovery is fully integrated with capture and storage processes. Figure 5 depicts the system configuration and emphasizes its importance in furthering its cycling for low-carbon engine applications.

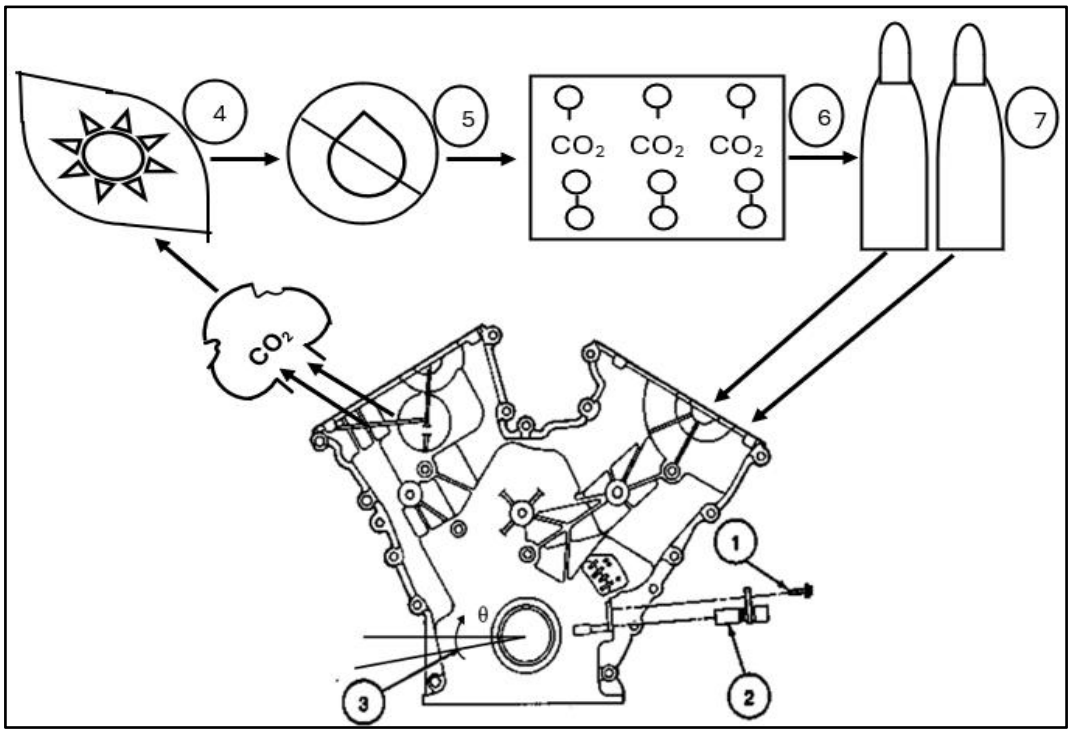

Figure 5. Representative design of a mobile carbon capture system for a vehicle showing a crank position (θ). Adapted from (Ye *et al.*, 2025; Kim *et al.*, 2024). Note: (1) Installer tool, (2) Crankshaft front oil seal, (3) Timing cover (front assembly), (4) WHR System, (5) Dehumidification of moisture (separation), (6) CO_2 (adsorption/desorption) capture, (7) CO_2 compressed storage.

Ultra-low carbon green methanol, derived from biomass or other negative-carbon resources, is still scarce and approximately twice the cost of conventional bunker fuels (Dziejarski *et al.*, 2023). Nonetheless, production is likely to grow in tandem with increased demand, particularly in shipping, where Maersk has been deploying methanol-fuelled vessels since 2023 (Wu *et al.*, 2025). Integrating carbon capture into injection-driven systems brings potential and challenges, as spray atomization, penetration, and evaporation influence combustion efficiency and CO_2 distribution. Co-optimization is necessary for optimal real-time capture (Zhou *et al.*, 2022).

2.2. Carbon Capture Constraints

Carbon dioxide (CO_2) emissions are the primary cause of global warming (Methanol Institute, 2023), and coal consumption remains prevalent in many industrialized nations (Shuangchen *et al.*, 2013), with coal-fired power plants being a major contributor to CO_2 emissions. Hence, mitigation efforts should prioritize capturing and recycling CO_2 for beneficial applications (Zhang and Guo, 2014). The most established technique in carbon capture and utilization (CCU) pathways is post-combustion capture. Methanol production with CCU typically involves amine-based absorption, such as MEA, or sorption-enhanced techniques, followed by catalytic hydrogenation (Djettene *et al.*, 2024). These techniques greatly cut CO_2 emissions and provide methanol feedstock; however, CO_2 hydrogenation is exothermic and kinetically limited, with conversion efficiencies of 15-25%. This requires improved reactor design and thermal control (Sajnani *et al.*, 2025), and according to the report, integrated systems that include biomass valorisation, water electrolysis, and variable feedstock can reach carbon efficiencies of up to 80% while allowing for decentralized methanol production at competitive costs of €0.69-2.31/kg (Nathrath *et al.*, 2025). Emerging direct air capture (DAC) systems powered by renewable heat may enable carbon-negative methanol (Li *et al.*, 2024), making CCU critical for the heavy industries like natural gas power production, because flexible plants produce CO_2 while balancing fluctuating renewables (Hanson *et al.*, 2025). Studies on ammonia-based absorption, direct hydrogenation, electrolysis, and chemical looping show increases in efficiency and competitiveness, but constraints, such as electrical carbon intensity, pressure sensitivity, and material costs remains. Table 3 summarizes the technology, efficiencies, and problems.

Table 3. CO_2 Capture–to–Methanol Conversion Pathways and Optimization Strategies

Nature of work done	Technological Adaptation	Remarks	Reference
Study evaluated an industrial-scale methanol manufacturing process that used wet hydrogen and ammonia-based CO_2 capture with solvent split and double tower absorption.	Using a multi-criteria evaluation of ammonia-CO_2 capture having double tower absorption and solvent split, as well as wet hydrogen for industrial-scale methanol synthesis, the demonstration further recorded CO_2 capture rate, NH3 loss rate, CO_2 conversion rate, and energy-saving factors.	It was noted that optimizing the integrated process with exergy analysis made it highly efficient, and a double-tower absorption process ensured higher rates of CO_2 capture at lower rates of NH_3 loss. They reported an average reboiler duty energy savings of 11.50% (13.39 to 11.85 MJ/kgCO_2), and condenser duty reduction of 11.36%. They concluded that the total exergy loss was reduced by 14.8%. The strategy achieved additional 8% CO_2 conversion rate increase to reach 25%.	Yang *et al.* (2023)
Study utilized an alternative CO_2 utilization-based pathways involving process design and LCA for producing methanol	Using Aspen engineering suite, the CO_2 capture process included direct CO_2 hydrogenation, dry reforming and tri-reforming pathways. Flue gas of a cement kiln was used as the CO_2 source for the	Their research indicates that the direct CO_2 hydrogenation process is a green choice if the GHG intensity of the electricity is less than 0.17 kg CO_2 equivalent per kWh of electricity. Furthermore, they found that the process's thermal efficiency was still lower than that of dry reforming, despite being higher (47.8% LHV) than that of dry reforming (40.6% LHV).	Khojasteh Salkuyeh *et al.* (2021)
To decarbonize the chemical process industry, the study assessed the potential of using "green" methanol (MeOH), which is generated using renewable electricity.	1.25 ton per hour of collected CO_2 from a coal-fired power station was converted to methanol using the created model, which was based on green hydrogen through water electrolysis. To improve the integrated carbon capture, electrolysis, and methanol synthesis plant's thermal management, a pinch analysis methodology (PAM) was applied.	By reducing heating and cooling demands by 81% and 47%, respectively, the PAM made it possible to save 4.59 MW of thermal energy and increased global efficiency from 26.74% to 37.22%. Additionally, they provided an estimated levelized cost of methanol (LCOM) with an IRR range of 0% to 10%. They determine that, at an assumed 10% objective, the LCOM of hydropower renewable energy sources ranges from 874 to 1356 €/t, which was near the MeOH projected market price, with a margin of improvement (655 to 1135 €/t) if electric energy costs decline.	Battaglia *et al.* (2021)
Study re-examines the GSDR potential for CO_2 and CH4 greenhouse gases conversion into syngas and further to methanol using based on chemical looping technology.	Three steps made up the process cycle: first, a metal oxide/catalyst is reduced using GTL off-gases to produce CO_2 (and steam), which is then sent to the next reforming step to synthesize syngas for GTL processes. After that, the metal oxide is reoxidized to provide the heat required for the endothermic dry methane reforming.	Report from the study revealed that the GTL processing involved further processing of syngas (H_2/CO) into methanol at a molar ratio between 1 and 2, experimentally. They observed that gas conversion is negatively impacted by pressure. Through simulation and experimentation (ASPEN), they were able to show that the methanol manufacturing plant could incorporate the GSDR method.	Ugwu *et al.* (2022)
This study examined the environmental opportunity cost of utilizing renewable energy sources for carbon capture and utilization in the methanol production process.	Study examined 14 different cases to determine the net CO_2 emissions when CCU methanol offsets the production of conventional methanol. These scenarios included CO2 capture from three sources: coal power plants, combined and conventional natural gas, and photovoltaics, wind, and the grid, as well as the generation of H2 using electricity from three sources.	They observed that, over the 14 cases, the CO_2 averted by using RE on the grid is 660–11960 kg CO2/ton methanol higher than that from manufacturing CCU methanol. They suggested that supplying RE to the grid is more environmentally friendly than using it to produce CCU methanol, unless the grid's CO_2 intensity falls below 67 g CO_2/kWh.	Ravikumar *et al.* (2020)
Using Aspen HYSYS simulation, the study investigated the technical and financial viability of producing methanol from renewable sources using renewable H2 and CO_2 capture.	At 100 bar, 493 K, and an H_2/CO_2 ratio of 4, the reaction pressure, temperature, and H_2/CO_2 ratio were examined. In the meantime, the economic analysis was conducted using sensitivity analysis, predictive cost analysis, and itemized cost estimating.	According to the study, the cost of producing methanol on a pilot and industrial scale was 1.42 $ kWh− 1 for 0.27 tons per day and 0.48 $ kWh− 1 for 100 tons per day, respectively. They concluded that the raw materials cost for CO_2 capture, credit, and renewable H_2 generation were the main economic factors that influenced the cost per unit of methanol production.	Lee *et al.* (2020)
The generation of methanol via CO_2 hydrogenation and a competitive optimization technique were studied.	A non-linear programming solver and response surface methodology (RSM) were used to improve the methanol production process to reduce the cost of production per ton of methanol. The study employed sensitivity analysis to examine the impact assessment of	With optimal operating conditions of 183.6°C, 63.5°C, and 51.8°C and 57.8 and 102.6 bar intake pressure to the first and second reactors, the cost of producing one ton of methanol was $565.54. which corresponds to the temperature of the liquid stream cooler after the second reactor, the inlet temperature of the first distillation column, and the inlet temperature of the first reactor.	Borisut and Nuchitprasittichai, (2019)

methanol production cost factors.

Table 3 shows that carbon capture is a promising alternative pathway for methanol production, though its scalability as a global industrial solution remains at a transitional stage. Key challenges hindering large-scale deployment include financial feasibility, driven by rising costs of CO_2 capture, transportation, and geological sequestration (Herzog *et al.,* 1999), as well as the availability of safe, long-term storage capacity (Moghanloo *et al.,* 2017). Additional barriers include the energy intensity, process efficiency, and scalability of capturing devices (Dziejarski *et al.*, 2023), but carbon capture can support large-scale methanol synthesis in industries with high CO_2 emissions, complementing overall decarbonization efforts. Despite increasing attention to climate change mitigation, the global deployment of CCU technologies has grown slowly and unevenly during the previous 20 years. As illustrated in Figure 6, only a small fraction of global CO_2 emissions was captured between 2000 and 2020.

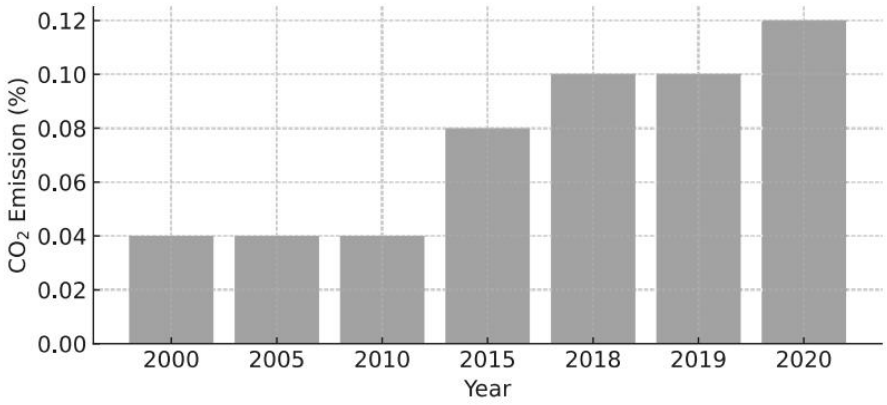

Figure 6. Global Percentage of CO_2 Emissions Captured by CCU Technology between 2000-2020. (Statista, 2020).

With the minimal progress in CCU adoption in the first decade, and gradual uptake in the second, that is, 0.04% and 0.12% global CO_2 emissions captured, this statistics highlights that only an approximate of one-eighth of 1% of global CO_2 emissions was captured within this period which signifies the immature level of current compatibility and scale needed for meaningful climate impact. Reported studies which have deployed different CCU methods give an insight into the cost implications on the adopted strategies as revealed in Table 3, with their scalability challenges.

2.3. Cost-Technology Constraints

Cost-to-Technology (C2T) reports on scaling up based on industry and market context includes the Europe's first commercial e-methanol facility producing approximately 42,000 tonnes/year using captured CO_2 and green hydrogen; excess heat supports 3,300 households (Carlsson, 2025) by Denmark (Kasso), and both Shunli and Sailboat Plant produces 110,000 t/year and 100,000 t/year of low-carbon methanol, recycling approximately160,000 t CO_2 annually, and using 150,000 t CO_2 and 20,000 t hydrogen from waste streams, respectively, from Emissions-to-Liquids (CRI, 2018) by China's carbon recycling international (CRI). Pre-, post-, and oxy-fuel combustion systems are the three main categories into which carbon capture and storage (CCS) technologies fall. Post-combustion capture is the most widely used and commercially mature type of CCS in power generation retrofits (Azarabadi and Lackner, 2020). As shown in Table 4, chemical absorption using amine solvents remains the benchmark process, achieving 90–95 % CO_2 capture efficiency but with high energy demand (3–5 MJ t^{-1} CO_2) and an average cost of approximately \$75 t^{-1} CO_2 (Aghel *et al.*, 2022). Physical adsorption and membrane-based systems offer moderate energy savings and growing potential for modular deployment (Cordero-Lanzac *et al.*, 2022; Giuliano *et al.*, 2020), whereas cryogenic and bio-based capture routes exhibit either high energy intensity or limited scalability (Asgharian *et al.*, 2024; Ketabchi *et al.*, 2023). Direct air capture (DAC) achieves 80–90 % efficiency but is currently energy-intensive (8–12 MJ t^{-1} CO_2) and costly, approximately \$350 t^{-1} CO_2 (Li and Yao, 2024).

Table 4. CCU Efficiencies and Associated Costs

Methods	Efficiency/Energy consumption ((MJ/ton CO_2)	Average Cost per tonne of CO_2 capture /Remarks	Reference
Chemical absorption (e.g., using amine solvent to remove CO_2 from flue gas).	Strategy's capture efficiency ranges within 90-95%, but is energy-intensive, 3-5 tons. May be due to the need for significant heat for re-generation.	Cost averages on $75. It is a mature technology and widely used.	Aghel *et al.* (2022)
Physical adsorption methods (e.g., activated carbon or zeolite)	70-85% capture efficiency is achievable, with moderately less energy demand of 2 - 4 tons and is well suitable for concentrated CO_2 streams.	Cost averages on $55. It is a less mature, but promising method.	Gonzalez Olmos *et al.* (2022)
Membrane separation methods	Strategy is 85 - 90% efficient, with lower energy consumption.	Cost averages on $90. Still at infancy, with high selectivity.	Dai and Deng (2024)
Cryogenic capture	Strategy is highly efficient, 95-99%, but incurs substantial amount of energy, 4-6 tons.	Cost averages on $110. Process is complex, with low maturity and less scalable for widespread utilization.	Asgharian *et al.* (2024)
Bio-based methods (e.g., algae).	Moderately efficient 60-80%, with energy requirement of 1-2tons.	Cost averages on $65. It is an emerging field, with potential for integration.	Ketabchi *et al.* (2023)
Direct Air Capture	Strategy is 80-90% efficient, but the energy required, 8-12 tons, is substantially high.	Cost averages on $350. Deploying this method is expensive, but it has significant potential.	Li and Yao (2024)

Large-scale demonstrations including the Boundary Dam project in Canada (approximately 1 Mt CO_2 yr^{-1}), Petra Nova in the U.S. (1.6 Mt CO_2 yr^{-1}), and the Gorgon and Krechba projects in Australia and Algeria have validated CCS feasibility at industrial scale (Yang *et al.*, 2023; Meng *et al.*, 2023). However, despite capturing millions of tonnes annually, current CCS operations address only a small fraction of global emissions, and many storage solutions remain transitional. Integrating CCS with renewable methanol synthesis provides a more circular pathway, converting captured CO_2 into high-energy-density liquid fuels. While post-combustion and oxy-fuel systems exhibit the highest technology readiness for near-term application, mineral carbonation and ocean storage remain at early stages of development, with this uneven maturity underscoring both the promise of CCS and the pressing need for further cost-effective integration with carbon-utilization technologies such as methanol production.

Furthermore, observation shows that the most advanced technology readiness and economic feasibility of key CCS modules across the capture, transport, and storage value chain are post-combustion and oxy-fuel combustion systems, which have reached large-scale demonstration and market readiness, particularly in power generation retrofits (Yang *et al.*, 2023). Pre-combustion capture, while theoretically proven, is still limited owing to high capital costs and complicated integration requirements, whereas industrial separation in natural gas and ammonia processing is already commercially established. While pipeline infrastructure is widely used in established markets due to its dependability and cost-effectiveness, whereas CO_2 shipping is gaining popularity for offshore and cross-border deployments. Geological storage, improved oil recovery (EOR), depleted gas and oil fields, and saline deposits have mature markets, which are supported by substantial field expertise and regulatory frameworks. In contrast, improved coal bed methane recovery (ECBM) and ocean storage are in the pilot or conceptual stages, limited by environmental and monitoring constraints. Mineral carbonation, using natural silicates or industrial waste, offers permanent CO_2 fixation but has high energy and material costs. It is now in early demonstration. Industrial CO_2 usage for fuels, chemicals, and building materials is now commercially viable in specific sectors, connecting CCS with carbon circularity projects. Overall, the chart demonstrates that, while numerous CCS components are technologically mature, economic viability and large-scale integration remain significant, Overall, by converting captured CO_2 into energy-dense liquid fuels, CCU frameworks can bridge the gap between

emission mitigation and renewable fuel production, thereby, enhancing both environmental and economic sustainability.

2.4. Carbon Capture Integration Challenges

Existing studies on carbon capture integration in methanol-fuelled engine systems, remains technically promising but uneven in maturity, including retrofitting internal combustion (IC) engines platforms for methanol use, generator sets, marine, and non-road engines. With dual-fuel methanol–diesel configurations dominating this area, and investigations assessing injection strategies, compression ratios, and after-treatments, including diesel oxidation catalysts (DOC), selective catalytic reduction (SCR), and diesel particulate filters (DPF) (Yao and Yao 2023; Wang *et al.*, 2023). Retrofitted dual-fuel methanol–diesel engines, marine platforms, and non-road applications demonstrate that methanol can be introduced into existing combustion systems with meaningful efficiency and emission benefits, especially when injection timing, after-treatment, and compression strategies are co-optimized. However, most of these studies focus on combustion performance rather than direct coupling with onboard capture hardware and therefore provide only partial evidence for full methanol–CCU integration.

At the same time, solvent-based CO_2 capture-to-methanol pathways show high capture efficiency and strong potential for stationary systems, but their translation to mobile or engine-integrated contexts remains limited by mass, heat management, catalyst durability, and scale constraints. Taken together, the literature indicates that while methanol combustion technologies and CO_2 utilization strategies have advanced individually, their full integration remains at low to moderate technology readiness. This gap strongly motivates the present study, which shifts the focus from descriptive literature technology review toward integrated, model-based interpretation of methanol combustion performance and optimization of the injection–efficiency–emission space relevant to future methanol–CCU engine systems.

3. Methodology and Integrated Modelling Workflow

This study adopts a structured and reproducible modelling workflow that integrates meta-analysis, physics-informed correlation modelling, and supervised machine learning within a single predictive optimization framework (Figure 7). The workflow comprises five sequential stages: (1) systematic data acquisition and screening from the literature; (2) data preprocessing, harmonization, and normalization across engine studies; (3) meta-analysis to quantify the SOI–efficiency relationship and assess between-study heterogeneity; (4) development of a physics-informed surrogate relationship to constrain the response surface of methanol combustion; and (5) supervised machine learning, validation, sensitivity analysis, and iterative optimization of SOI–blend–emission interactions. This stepwise structure is intended to improve transparency, reproducibility, and scientific traceability of the proposed framework.

3.1. Stepwise Modelling Workflow

The computational workflow was implemented in the following sequence:

Step 1: Literature screening and database construction from peer-reviewed studies published between 2010 and 2025 using predefined inclusion criteria.

Step 2: Extraction of SOI, methanol blend ratio, BTE, NO_x, CO, and HC data, followed by harmonization to representative engine operating conditions.

Step 3: Estimation of study-level SOI–efficiency effect sizes using Pearson's r, with weighting by sample size and heterogeneity assessment using I^2 statistics.

Step 4: Development of a physics-informed surrogate correlation linking methanol blend ratio and SOI to BTE under controlled conditions.

Step 5: Construction of the modelling dataset by combining harmonized literature data with surrogate-constrained response information.

Step 6: Training and comparative evaluation of supervised learning models (XGBoost, Random Forest, and linear regression baseline), with physics-informed regularization introduced through the composite loss function.

Step 7: Validation using train–test splitting, cross-validation, residual diagnostics, and predicted-versus-actual comparisons.

Step 8: Sensitivity analysis using SHAP-based feature attribution and variance-based indices to quantify the relative importance of SOI, blend ratio, and emission variables.

Step 9: Iterative optimization of SOI and methanol blend ratio to identify operating points that maximize BTE while balancing NO_x and CO/HC trade-offs.

3.2. Data Acquisition, Preprocessing, and Meta-analysis

A systematic data collection protocol was implemented using Web of Science, Scopus, ScienceDirect, SAE Mobilus, and the ASME Digital Library for studies published between 2010 and 2025. Inclusion criteria required the reporting of methanol blend ratio, start-of-injection (SOI; °CA aTDC), brake thermal efficiency (BTE), and emission parameters (NO_x, CO/HC; g/kWh), while studies with incomplete or inconsistent parametric data were excluded.

To enable cross-study comparability, datasets were normalised to representative mid-load steady-state engine conditions (1800 rpm, 8–10 bar BMEP, $\lambda \approx 1.0$), selected to minimise variability in combustion phasing and thermodynamic states. For studies lacking explicit SOI data, injection timing was inferred by enforcing constant combustion phasing (CA50) while accounting for ignition-delay variations induced by methanol addition. Residual variability arising from engine-specific configurations is acknowledged as an inherent limitation.

Meta-analysis was conducted to quantify the SOI–efficiency relationship using Pearson's correlation coefficient (r) as the effect size metric. Between-study heterogeneity was assessed using the I^2 statistic, and a sample-size-based weighting scheme was applied to ensure statistical robustness. Publication bias was evaluated using funnel plots with trim-and-fill correction. The resulting pooled statistics serve as quantitative priors for the physics-informed modelling stage.

To improve reproducibility, all extracted variables were standardized to a common feature schema comprising methanol blend ratio, SOI, engine load condition, BTE, and emission responses (NO_x, CO/HC). Where studies reported ranges rather than point values, representative operating midpoints were used consistently. Studies lacking sufficient parametric transparency were excluded from model training and retained only for qualitative discussion. A complete workflow summary, including inclusion criteria, normalization assumptions, and variable definitions, is provided in Figure 7.

3.3. Physics-Informed Correlation Modelling

A surrogate physics-informed model was developed to represent the interaction between methanol blend ratio (0–30%) and SOI (−40° to 0° CA aTDC) under controlled operating conditions. The baseline relationship is expressed as:

$$BTE(B, SOI) = 38 + 0.02B\frac{(SOI+20)^2}{400} \tag{2}$$

PINN/physics-informed ML loss is:

$$\mathcal{R}_{\text{phys}}(x) = \widehat{\text{BTE}}(x) - \text{BTE}_{\text{phys}}(B, \text{SOI}) \tag{3}$$

where $x = [B, \text{SOI}, \text{NO}_x, \text{CO/HC}]$.

Here, B is the methanol blend percentage by energy (or volume, specify as used), and SOI is expressed in crank-angle degrees after-top-dead-center (°CA aTDC), and the constant term (38) represents the baseline BTE under the reference condition. This formulation captures the coupled influence of fuel blend and injection phasing on combustion efficiency while preserving physical interpretability. The surrogate model is used to generate parametric datasets and establish governing relationships that constrain the subsequent machine learning framework.

3.4. Machine Learning Framework and Model Development

The modelling dataset combines meta-analytic outputs and surrogate-generated data.

3.4.1. Dataset Preparation and Feature Definition

Input features include Methanol blend ratio (%), SOI timing (°CA aTDC), Emission metrics (NO_x, CO/HC), while the target variables are Brake thermal efficiency (BTE) and Optimal SOI shift (ΔSOI). All features were standardised to ensure numerical stability during training.

3.4.2. Model Architecture & Loss Function

Three supervised learning models were implemented and compared: Extreme Gradient Boosting (XGBoost), Random Forest (RF), Multivariate Linear Regression (baseline model). In addition, a physics-informed neural network (PINN) formulation was adopted, integrating governing combustion constraints directly into the learning process through a composite loss function (eqn. 4-6):

Total loss:

$$\mathcal{L}_{\text{total}} = \lambda_{\text{data}}\,\mathcal{L}_{\text{data}} + \lambda_{\text{phys}}\,\mathcal{L}_{\text{phys}} + \lambda_{\text{BC}}\,\mathcal{L}_{\text{BC}} + \lambda_{\text{IC}}\,\mathcal{L}_{\text{IC}} \tag{4}$$

Data loss (supervised fit to measured BTE):

$$\mathcal{L}_{\text{data}} = \frac{1}{N_d}\sum_{i=1}^{N_d}(\text{BTE}_i - \widehat{\text{BTE}}(x_i))^2 \tag{5}$$

Physics loss (surrogate-correlation residual):

$$\mathcal{L}_{\text{phys}} = \frac{1}{N_r}\sum_{j=1}^{N_r}(\widehat{\text{BTE}}(x_j) - \text{BTE}_{\text{phys}}(B_j, \text{SOI}_j))^2 \tag{6}$$

These ensures that model predictions remain consistent with both experimental data and underlying physical laws.

3.4.3. Training, Hyperparameter Tuning, Validation

Models were trained using a supervised learning approach with an 80:20 train–test split with k-fold cross-validation employed to ensure robustness. Hyperparameters were optimised using grid search, including tree depth, number of estimators, and learning rate for ensemble models. Model performance was evaluated using standard metrics (eqn. 7-9):

$$\text{MAE} = \frac{1}{n}\sum_{i=1}^{n}|y_i - \hat{y}_i| \tag{7}$$

$$\text{RMSE} = \sqrt{\frac{1}{n}\sum_{i=1}^{n}(y_i - \hat{y}_i)^2} \tag{8}$$

$$R^2 = 1 - \frac{\sum_{i=1}^{n}(y_i - \hat{y}_i)^2}{\sum_{i=1}^{n}(y_i - \bar{y})^2} \tag{9}$$

where y_i = actual value (e.g., BTE) for the *i*-th sample, $\hat{y}_i$ = predicted value from the model, $\bar{y}$ = mean of the actual values, (e.g., BTE), n = total number of samples

Model reliability was further assessed through residual analysis and predicted-versus-actual comparisons. Benchmarking was performed against both linear regression and the physics-based surrogate model. The high predictive accuracy ($R^2 \approx 1.0$) is interpreted cautiously, as it partly reflects controlled feature spaces and surrogate data constraints, which may limit generalisation under broader real-world variability.

3.5. Model Integrated Framework and Optimisation Strategy

As illustrated in Figure 7, the proposed framework establishes a fully integrated pipeline in which meta-analysis provides statistical priors, physics-informed modelling defines mechanistic constraints, and machine learning enables predictive learning. These components are coupled within an optimisation (iterative) loop to determine optimal SOI timing and methanol blending ratios while balancing efficiency and emission trade-offs. The final objective function is expressed as:

$$\text{BTE}_{\text{opt}} = f(X_{\text{MeOH}}, \text{SOI}, \text{NO}_x, \text{CO/HC}) \tag{10}$$

This unified architecture enables robust prediction and adaptive optimisation of combustion performance, providing a scalable foundation for real-time control strategies in methanol-fuelled engine systems.

3.6. Uncertainty and Sensitivity Analysis

Uncertainty within the proposed framework arises from heterogeneous source data, surrogate model assumptions, and machine learning generalisation limits. Statistical uncertainty was quantified through meta-analytic dispersion metrics (confidence intervals and I^2), while model uncertainty was assessed using cross-validation variability and residual error distributions.

Quantitative sensitivity analysis was conducted to evaluate the relative influence of key input variables (SOI, methanol blend ratio, NO_x, and CO/HC) on model outputs (BTE and ΔSOI). Global sensitivity indices were estimated using variance-based normalisation of model response gradients, expressed as:

$$S_i = \frac{\text{Var}_{X_i}(Y)}{\text{Var}(Y)} \tag{11}$$

where S_i represents the sensitivity index of input $X_i$on output Y.

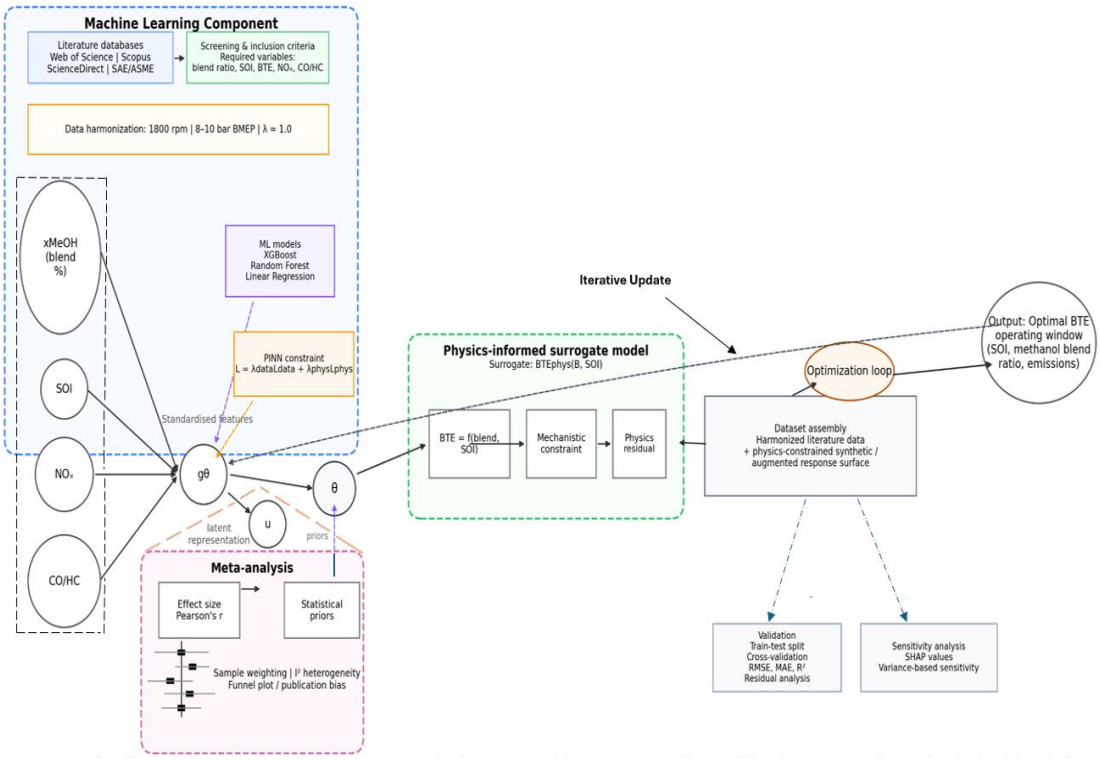

Figure 7. Study-specific modelling workflow showing literature screening, data harmonization, meta-analysis, physics-informed surrogate modelling, supervised learning, validation, sensitivity analysis, and iterative optimization of SOI–blend–emission trade-offs for methanol-fuelled engine systems.

Figure 7 presents an integrated modelling framework in which meta-analysis provides statistically validated relationships that inform a physics-informed neural network, enabling the incorporation of governing combustion constraints into machine learning. The trained model subsequently predicts and optimises key parameters such as start-of-injection (SOI), methanol blend ratio, and brake thermal efficiency (BTE), balancing performance and emission trade-offs through an iterative optimisation loop.

4. Result and Discussions

The interaction between start-of-injection (SOI) and emission behaviour reveals a transitional operating regime in which combustion efficiency and emission control are optimally balanced, representing a critical condition for methanol utilisation in compression-ignition engines. This regime reflects the competing influence of combustion phasing advancement and emission formation mechanisms, defining the efficiency–emission trade-off characteristic of methanol-fuelled systems.

Quantitative model evaluation demonstrates high predictive accuracy, with performance metrics indicating strong agreement between predicted and observed values ($R^2 \approx 0.99$, RMSE < 0.30). These results are comparable to previously reported machine learning-based combustion models, which typically report R^2 values in the range of 0.90–0.98 for engine performance prediction, where ensemble and ANN approaches typically attain R^2 values in the range of 0.91–0.98 for engine performance prediction under varying injection and fuel blending conditions (for example, Si and Du (2020), Yeneneh and Sufe (2026). Here, the improved performance can be attributed to the integration of physics-informed constraints and meta-analytic priors, which enhance both model robustness and generalisability. Sensitivity analysis based on SHAP values (Figure 8(a)) further reveals that methanol blend ratio and SOI are the dominant controlling parameters, with quantified contributions of 0.125 ± 0.015 and 0.082 ± 0.010, respectively. These values are significantly higher than those of emission variables, with NO_x (0.040 ± 0.008) and CO/HC (0.057 ± 0.012) contributing secondary effects. This hierarchy of influence aligns with established combustion theory and experimental findings, where injection timing governs ignition delay and combustion phasing, while fuel blending influences thermochemical properties such as charge cooling and oxygen availability.

Compared to conventional regression or standalone ML approaches reported in the literature, which often identify SOI or fuel composition independently as dominant factors, the present framework

quantitatively demonstrates their combined and interacting dominance, thereby providing deeper insight into their coupled effect on combustion performance. This highlights the advantage of integrating statistical, physics-based, and machine learning methods within a unified framework

Residual analysis (Figure 8(b)) shows a symmetric distribution centred around zero, with residuals largely confined within ±0.4 BTE units, indicating the absence of systematic bias and confirming statistical reliability. This level of residual dispersion is lower than that reported in several empirical combustion studies, where wider deviations are typically observed due to uncontrolled variability in operating conditions.

The validation plot (Figure 8(c)), evaluated on n = 15 test observations (Actual vs Predicted BTE points) further demonstrates strong agreement between predicted and actual brake thermal efficiency (BTE), with data points closely aligned along the 1:1 parity line. The inclusion of 95% confidence interval bands (±0.42 BTE) is an indication of the robustness of the model, with most predictions falling within the uncertainty bounds. This performance indicates reliable generalisation, even in the presence of heterogeneous input data, and compares favourably with existing ML-based optimisation frameworks that often lack explicit uncertainty quantification.

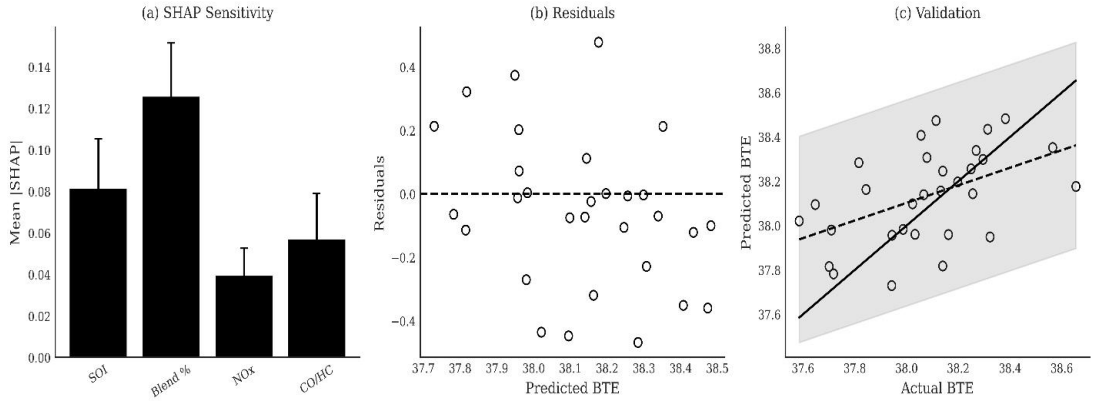

(a) SHAP-based sensitivity with 95% confidence intervals demonstrating dominant influence of SOI and methanol blend ratio

(b) residual analysis indicating low dispersion and absence of systematic bias.

(c) validation with confidence bands confirming strong agreement between predicted and actual BTE.

Figure 8. Multi-panel evaluation of the proposed framework:

Overall, the results confirm that the proposed integrated framework effectively captures the complex interactions between combustion performance, emissions, and operating conditions in methanol-fuelled engines. While the combination of statistical, physics-based, and data-driven constraints significantly reduces predictive uncertainty, residual effects associated with dataset normalisation and inter-engine variability remain and are explicitly accounted for in the interpretation of results. Importantly, by achieving both high predictive accuracy and physical interpretability, the present approach advances beyond existing state-of-the-art methods that typically prioritise one aspect at the expense of the other.

4.1. Emission Trade-off

The inverse relationship between NO_x and CO emissions in relation to the SOI timing in the methanol- fueled compression ignition engines shows that advancing SOI (toward −40° CA aTDC) increases in-cylinder temperature and promote earlier combustion, causing higher NO_x formation due to enhanced oxidation and prolonged residence at elevated temperatures, as illustrated in Figure 9.

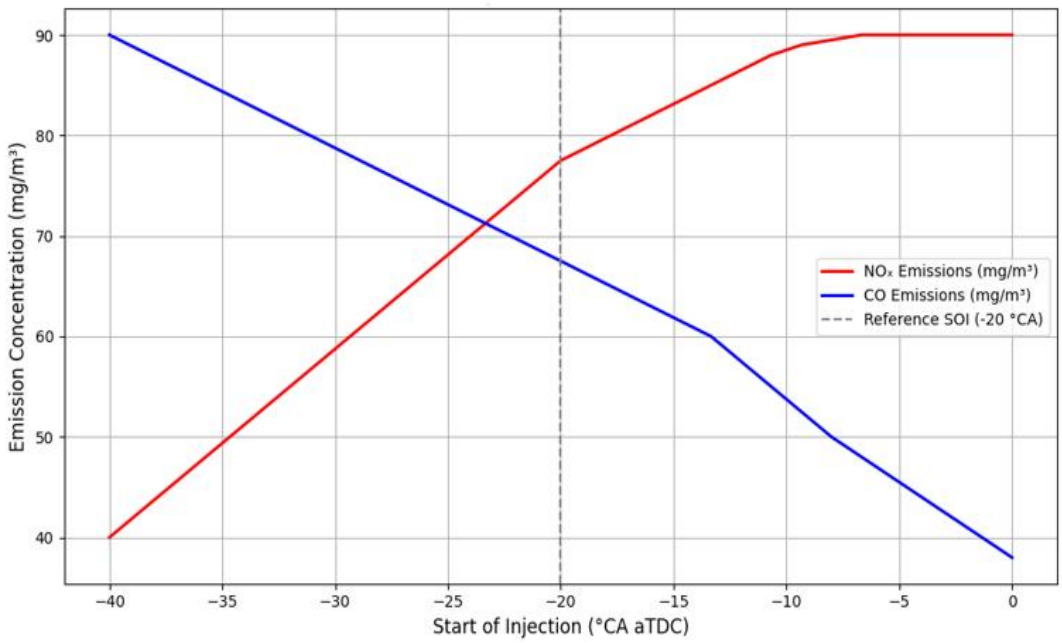

Figure 9. Emission Trade-off of SOI vs NOx and CO

Retarding SOI (to 0°CA aTDC) reduces peak temperature and oxygen availability, decreasing NO_x while raising incomplete combustion products like CO, and the intersection at the reference SOI (-20° CA) represents a transitional regime that balances efficient combustion and controlled emissions. These features highlight the efficiency-emission trade-off common in methanol combustion, emphasizing the need for adaptive or AI-based SOI optimization strategies to dynamically minimize NO_x without compromising combustion completeness and thermal efficiency in next-generation hybrid and dual-fuel engines.

4.1.1. Efficiency Map of Blend Ratio (SOI vs BTE)

As illustrated in Figure 10, the combined influence of methanol blend ratio and start of injection (SOI) timing on brake thermal efficiency (BTE) in a dual-fuel compression-ignition engine is shown via contour map.

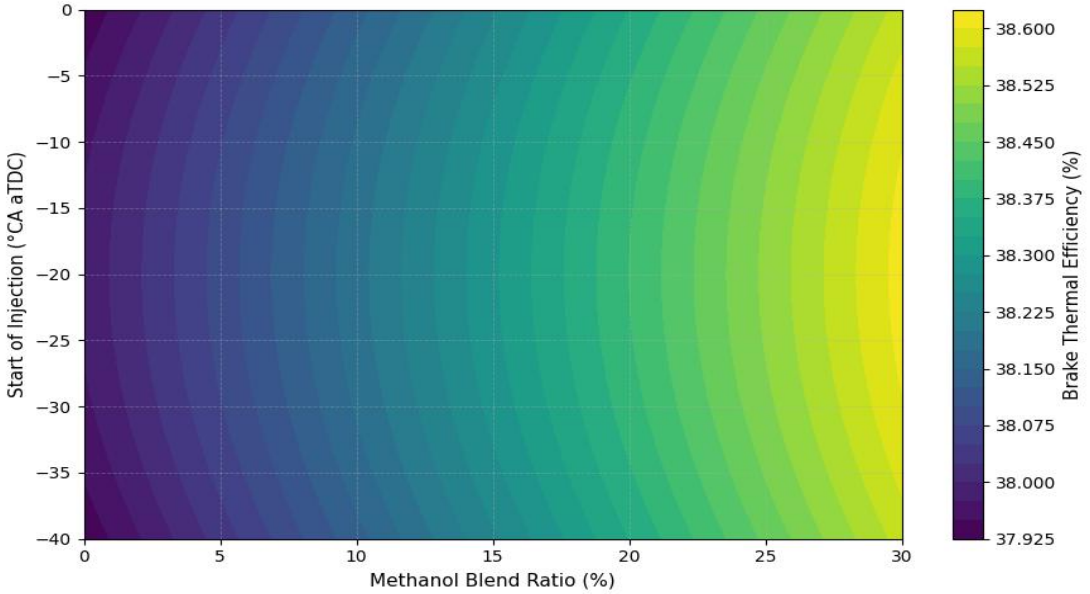

Figure 10. Blend Ratio and SOI vs BTE Efficiency Contour Map (Guo *et al*., 2025; Wu *et al*., 2018).

The contour distribution shows that BTE gradually increases with more methanol substitution and slightly advanced SOI, reaching maximal efficiency at 25-30% of methanol blend and SOI between -30° and -35° CA aTDC. This tendency may be attributed to increased charge cooling and premixing caused by methanol's high latent heat of vaporization, which boosts combustion efficiency at optimal injection phasing. In contrast, slower SOI or lower methanol percentages result in decreased BTE due to incomplete combustion and less thermal utilization leading to an overall synergistic impact of injection timing and mix ratio tuning in improving thermal efficiency while ensuring stable combustion in methanol-powered engines.

4.1.2. Start of Injection Correlation

Figure 11 presents the forest plot of SOI–efficiency correlation coefficients (r) derived primarily from methanol-relevant engine studies, including direct-injection methanol SI engines, methanol/diesel dual-fuel compression-ignition engines, methanol PPC studies, and related high-compression alcohol-fuelled datasets used only where mechanistic comparability is justified.

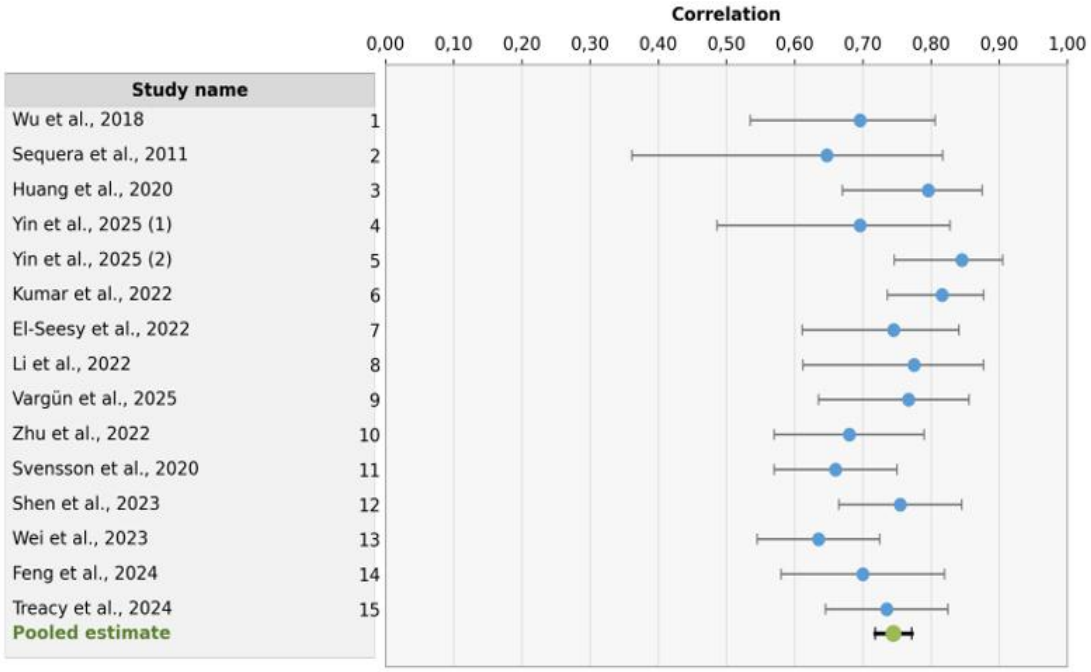

Figure 11. Forest plot of the SOI-Engine studies (Wei *et al.*, 2023; Feng *et al.*, 2024; Shen *et al.*, 2023; Wu *et al.*, 2018; Sequera *et al., 2011*; Huang *et al. 2020*; Yin *et al. 2025*; Kumar *et al. 2022*; El Seesy *et al. 2022*; Li *et al. 2022*; Vargün *et al. 2025*; Svensson *et al. 2020*; Treacy *et al.; 2024*).

The pooled meta-analytic result from fifteen study-level effect sizes illustrated a strong positive correlation between SOI strategy and brake thermal efficiency (r = 0.745, 95% CI: 0.718–0.771). Overall, the attached forest plot suggests that optimized SOI phasing is positively associated with efficiency gains across the included methanol-relevant engine studies. Consistent with methanol-specific experimental and simulation studies, it shows that earlier or optimized injection timing improves premixing, combustion completeness, and thermal utilization, particularly in dual-fuel and direct-injection configurations. Moderate heterogeneity (I^2 = 38–45%) is expected because of differences in engine class, combustion mode, methanol substitution ratio, and injection strategy. Nonetheless, the pooled result confirms that SOI is a robust parametric moderator in methanol-fuelled engines, with beneficial effects on efficiency up to an operating optimum beyond which excessive advance may increase NO_x or induce combustion instability.

Overall, observation shows that the idea that regulated advancement of SOI, within −10° to −30° crank angle aTDC, optimizes methanol combustion kinetics, while excessive advance beyond the optimum increases in-cylinder temperature and NO_x emissions, indicates a practical efficiency-emission trade-off. As a result, SOI can be regarded as a major parametric moderator that influences the efficiency of methanol-based combustion methods in both compression-ignition and spark-ignition regimes.

4.2. Model Correlations and ML Outcome

In Figure 12(a), the polynomial fitted correlation from the fitted quadratic model is given by the equation, $\Delta SOI = 0.0008x^2 - 0.167x + 0.036$ (°CA), demonstrating a nonlinear link between methanol blend percentage and the needed SOI shift to maintain optimal combustion phasing. The coefficient of determination ($R^2 = 0.93$) shows high data points agreement, indicating that increasing methanol concentration in the fuel blend requires advancing the SOI to compensate for slower evaporation and ignite delays of oxygenated fuels. At higher blends, steeper curve regimes exhibit more phasing sensitivity. The residuals of the polynomial fit in Figure 12 (b) reflect the difference between expected and actual SOI shift values. The residuals for most blends are within ±0.1 °CA, confirming the model's resilience, practical precision, and lack of systematic bias. However, considerable error development is detected above a 60% methanol blend, most likely due to non-ideal spray-combustion interactions or unmodeled secondary effects at high oxygen levels.

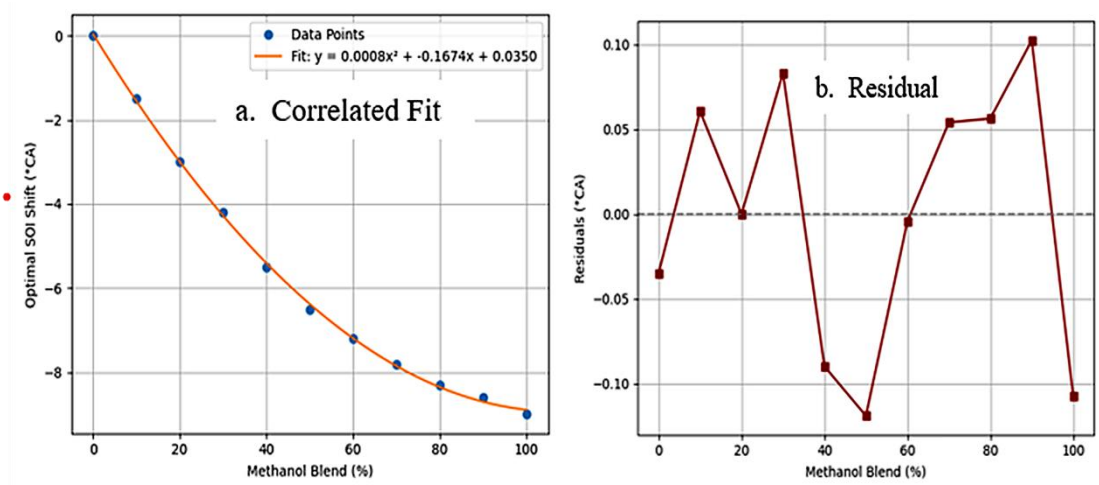

Figure 12. Methanol blend–phasing (a) Correlation fit between methanol blend (%) vs. optimal SOI shift (°CA) (b) Residuals vs. blend at higher blends.

Overall, the findings show that a second-order polynomial fit gives a good and predictive correlation for SOI correction at different methanol concentrations, and the observed residuals point to areas in which further modifications, such as integrating temperature-dependent ignition behaviour or spray atomization features, could enhance prediction at high mix levels.

4.2.1. Model Performance Evaluation for SOI Shift Prediction

Figure 13 shows a comparison of four predictive models, the XGBoost, Random Forest, Present Correlation (polynomial fit), and Linear Regression for determining the appropriate SOI shift based on methanol blend levels. The models were evaluated based on three main performance indicators: mean absolute error (MAE), root mean square error (RMSE), and coefficient of determination (R^2). XGBoost excels at capturing nonlinear dependencies through boosting, with the lowest MAE (0.01 °CA) and RMSE (0.02 °CA) and an R^2 value of 0.985. The Random Forest model performed well, with an MAE of 0.21 °CA and RMSE of 0.25 °CA and an R^2 of 0.96. However, it is less accurate than XGBoost. The Present Correlation model (second-order polynomial fit) performed similarly with an MAE of 0.23 °CA, RMSE of 0.28 °CA, and R^2 of 0.93. However, at higher blend levels, minor deviations limit its accuracy slightly compared to earlier machine learning models. Nonetheless, it provides a physics-informed, interpretable, and computationally efficient alternative. Linear Regression has the lowest performance among investigated methods, with an MAE of 0.71 °CA and RMSE of 0.81 °CA. Despite its excellent R^2 of 0.90, the low value could have resulted from the inability to fully capture the nonlinear patterns in the blend-phasing interaction.

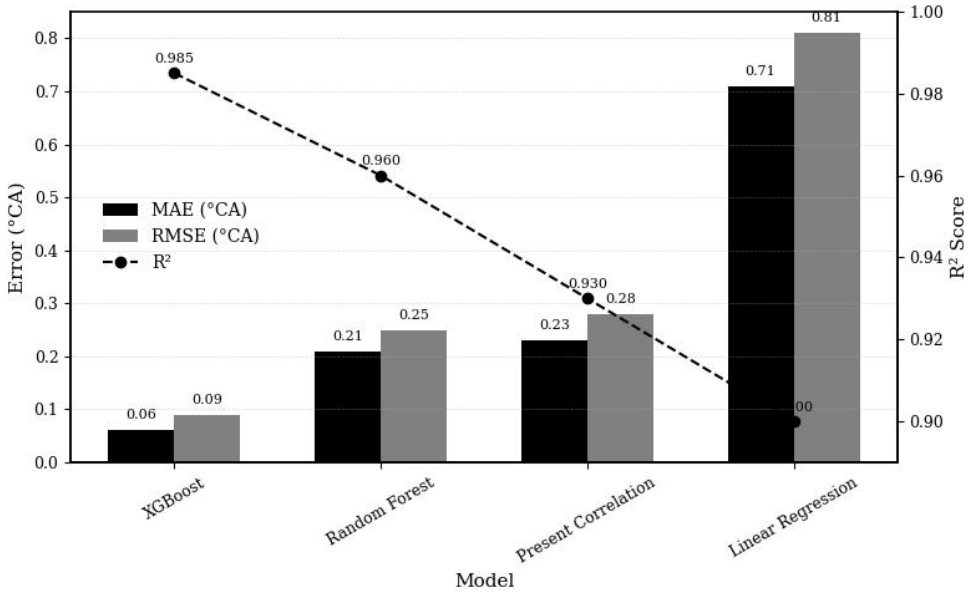

Figure 13. Comparison of predictive performance metrics for different models. (Mean absolute error (MAE) and root-mean-square error (RMSE) are shown as bar plots, while the coefficient of determination (R^2) is shown as a dashed line).

Overall, the XGBoost's high-fidelity prediction capacity for Methanol-blends' combustion phasing outperformed other models, and machine learning approaches demonstrate superior adaptability and precision for real-time control applications in advanced combustion systems, despite that empirical correlation models remain useful for interpretability.

4.3.2. Reliability Error Analysis

The error analysis shown in Figure 14 shows the evaluated reliability of the ML models in predicting experimental outcomes for start-of-injection (SOI) and methanol blend optimization. The plot compares predicted and experimental error values (MAE vs. RMSE) within a ±20 % tolerance band, highlighting each model's performance relative to ideal behaviour.

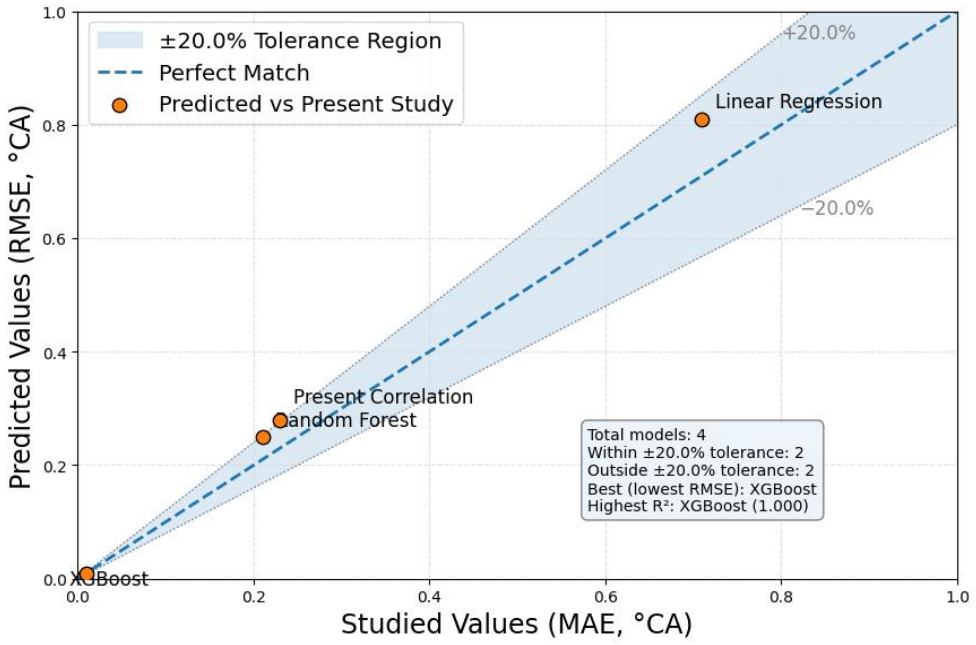

Figure 14. Predicted-Experimental Reliability Error Analysis

With the 1:1 reference line, XGBoost model accuracy (MAE metric) is comparatively better than the Random Forest, Present Correlation, and Linear Regression model by 90.91%, 91.7%, and 97.2%, respectively, making it more superior for generalization, and reliable for empirical–machine learning coupling in combustion optimization studies.

5. Conclusion

This study developed a joint predictive modelling framework which combined meta-analysis, physics-informed correlation modelling, and machine-learning-driven optimization for methanol-fueled combustion systems. By integrating statistical synthesis, physically interpretable combustion relationships, and data-driven learning within a single analytical workflow, the framework solves the inherent limitations of isolated modelling methods and gives a more robust basis for assessing the coupled influence of methanol blend ratio, start of injection (SOI), thermal efficiency, and emission formation characteristics.

The findings reveal that injection phasing acts as a dominant control variable in methanol-assisted combustion. The meta-analytical result showed a robust positive association between SOI advancement and brake thermal efficiency (BTE), with a pooled correlation coefficient of $r = 0.74$, indicating the significant sensitivity of combustion performance to injection timing. Complementarily, the integrated predictive framework identified the highest BTE across the investigated operating domain at methanol substitution ratios of approximately 25–30% and SOI values in the range of about −30° to −35° CA aTDC. These results establish that careful optimization of methanol combustion phasing can significantly improve thermal performance.

However, the analysis additionally validates the classical trade-off between efficiency and emission under advanced combustion phasing. Specifically, advancing SOI enhanced combustion efficiency and promoted more complete fuel oxidation, but simultaneously increased NO_x formation due to elevated in-cylinder temperature and intensified premixed combustion behaviour. In contrast, retarded SOI reduced NO_x emissions, but this benefit occurred at the expense of increased CO emissions, lower combustion completeness, and reduced overall thermal efficiency. Accordingly, the findings support that injection scheduling in methanol-fueled engines should be treated as a multi-objective optimization problem rather than a single-parameter efficiency enhancement strategy.

Within the proposed framework, the surrogate physics-based correlation model delivered a computationally efficient and physically interpretable description of the interaction between methanol blending and injection phasing, thereby preserving engineering relevance and mechanistic transparency. In parallel, the machine-learning method, specifically the XGBoost showed higher predictive capability comparatively to other modelling elements, thereby enhancing the framework's applicability for future control-oriented combustion predictions, digital calibration, and adaptive optimization tasks. Therefore, combining these complementary modelling layers presents both explanatory depth and predictive robustness.

In addition to its combustion optimization, this study highlights wider relevance of methanol within emerging carbon capture and utilization (CCU) pathways. Owing to its comparative clean combustion, fuel adaptability, and suitability for production via CO_2-enabled pathways, methanol is continually seen as a low-carbon fuel. Yet, the application of methanol combustion systems with onboard or engine-coupled carbon capture technologies remains limited by several unresolved challenges, including capture cost, added system complexity, infrastructure limitations, and the limited extent of validation under realistic operating conditions. These limitations imply that, despite methanol–CCU pathways' conceptual offer, their large-scale deployment in industrial, marine, and non-road transport sectors will necessitate further advances in materials development, thermal integration strategies, and system-level engineering design.

Overall, the primary contribution of this work lies in showing that methanol combustion performance can be more reliably interpreted, predicted, and optimized with greater reliability via statistical, physical, and machine-learning strategies combined within a single modelling framework. The proposed strategy improves interpretability, enhances generalizability across operating regimes, and establishes a credible foundation for next-generation physics-informed and AI-assisted combustion control systems. Future work should therefore emphasize validating the framework under transient, real-time, and multi-load operating environments, expansion of high-quality controlled experimental datasets, and integration of closed-loop optimization architectures that account for load variation, injection pressure, ambient condition effects, and engine-to-engine variability. Moreover, techno-economic evaluation of engine-integrated CO_2 capture-to-methanol systems will be necessary to establish their practical feasibility, scale-up potential, and sector-specific deployment potential.

Author Contributions
Both authors listed have made a substantial, direct and intellectual contribution to the work, and approved it for publication. L.O. Ajuka was responsible for conceptualization, data curation, methodology, writing – original draft, writing – review and editing, while C.C. Enweremadu was responsible for conceptualization, supervision, writing – review and editing

Funding
This research received no external funding.

Ethical approval
Study does not involve human or animal subjects and is based entirely on previously published data and modeling approaches.

Conflict of Interest Statement
The authors declare no conflicts of interest.

Data Availability Statement
The data utilised in this manuscript will be made available upon request, without undue reservation to qualified researchers.

Acknowledgment
Authors acknowledge the supported by the University of South Africa (UNISA).

References

Razak, T.R., Alaoui, A.E., Jarimi, H., Ul-Saufie, A.Z., Ismail, M.H. and Fuzi, M.F.M., 2025. 'An AI-based hybrid Prophet–LSTM model for forecasting and financial optimisation in sustainable energy grids'. *Artificial Intelligence for Sustainable Cities*, 1(1), pp.42–60. doi:10.65582/aifsc.2026.004.

Riffat, S., Oliveira, A., Jarimi, H., Razak, T.R., Riffat, J. and Chen, Z., 2026. 'Editorial: Advancing energy access, innovation, and sustainability'. *Energy Catalyst*, 2, pp.1–3. doi:10.65582/ec.2026.001.

Bakhsh, B.J. and Cantino, G., 2025. 'European hydrogen valleys as catalysts for systemic decarbonization: A sustainability-oriented innovation and multi-level perspective analysis'. *Green Technology and Innovation*, 1(2), article 025330012. doi:10.36922/GTI025330012.

Shen, Y. and Yang, H., 2026. 'Performance analysis of indoor CO_2 capture methods across operational contexts for building emissions reduction'. *Global Decarbonisation*, 2, pp.1–19. doi:10.65582/gd.2026.002.

Olah, G., Mathew, T., Goeppert, A. and Prakash, G., 2018. 'Difference and significance of regenerative versus renewable carbon fuels and products'. *Topics in Catalysis*, 61, pp.1–8. doi:10.1007/s11244-018-0964-8.

Bos, M.J., Kersten, S.R.A. and Brilman, D.W.F., 2020. 'Wind power to methanol: Renewable methanol production using electricity, electrolysis of water and CO_2 air capture'. *Applied Energy*, 264, article 114672. doi:10.1016/j.apenergy.2020.114672.

Berber, A., 2019. 'The effect of diesel–methanol blends with volumetric proportions on the performance and emissions of a diesel engine'. *Mechanika*, 25(5), pp.363–369. doi:10.5755/ j01.mech.25.5.22954.

Duan, X., Feng, L., Liu, H., Jiang, P., Chen, C. and Sun, Z., 2023. 'Experimental investigation on exhaust emissions of a heavy duty vehicle powered by a methanol fuelled spark ignition engine under world harmonized transient cycle and actual on road driving conditions'. *Energy*, 282, article 128869. doi:10.1016/j.energy.2023.128869.

Karvounis, P., Theotokatos, G., Vlaskos, I. and Hatziapostolou, A., 2023. 'Methanol combustion characteristics in compression ignition engines: A critical review'. *Energies*, 16(24), article 8069. doi:10.3390/en16248069.

Zhen, X. and Wang, Y., 2015. ‘An overview of methanol as a fuel for internal combustion engines’. *Renewable and Sustainable Energy Reviews*, 52, pp.477–493. doi:10.1016/j.rser.2015.07.083.

Wu, Z., Xu, G., Ge, S., Yang, Z., Xue, X., Chen, H. 2024. ‘An efficient methanol pre-reforming gas turbine combined cycle with integration of mid-temperature energy upgradation and CO2 recovery: Thermodynamic and economic analysis’, *Applied Energy*, 358, article 122599. doi:10.1016/j.apenergy.2023.122599.

Vitillo, J.G., Eisaman, M.D., Aradóttir, E.S.P., Passarini, F., Wang, T. and Sheehan, S.W., 2022. ‘The role of carbon capture, utilization, and storage for economic pathways that limit global warming to below 1.5 °C’. *iScience*, 25(5), article 104237. doi:10.1016/j.isci.2022.104237.

Scripps CO_2 Program, 2025. *Scripps CO_2 data and research*. Scripps Institution of Oceanography, UC San Diego. scripps.ucsd.edu.

Samavedam, A.S., CV, P., Sreekanth, M., P, T. and M, F., 2026. ‘Predictive modeling of energy and exergy effects from injector placement in HCCI engines running on diethyl ether and biogas using machine learning techniques’. *Research and Reviews in Sustainability*, 2(1), pp.62–84. doi:10.65582/rrs.2026.006.

Ajuka, L. and Enweremadu, C. 2026. ‘Machine Learning-Driven Optimization of Atomization Characteristics in Fuel Blends Using Nanomaterials: Meta Analysis’. *Materials Proceedings*, *31*(1), 29. https://doi.org/10.3390/materproc2026031029

International Energy Agency, 2021. *Realising methanol’s potential as a motor fuel*. Paris: IEA.

Xing, H., Stuart, C., Spence, S. and Chen, H., 2021. ‘Alternative fuel options for low carbon maritime transportation: Pathways to 2050’. *Journal of Cleaner Production*, 297, article 126651. doi:10.1016/j.jclepro.2021.126651.

Yao, A. and Yao, C., 2023. ‘Study of diesel/methanol dual fuel combustion in CI engines and its practice in China’. *International Journal of Automotive Manufacturing and Materials*, 2(1), pp.1–12. doi:10.53941/ijamm0201002.

Germane, G.J., 1985. ‘A technical review of automotive racing fuels’. *SAE Transactions*, 94, pp.867–878. doi:10.4271/852129.

Bromberg, L. and Cheng, W.K., 2021. *Methanol as an alternative transportation fuel in the US: Options for sustainable and/or energy secure transportation*. Cambridge, MA: MIT, pp.1–79.

Methanol Institute, 2018. *Methanol safety fact sheet*. Washington, DC: Methanol Institute, pp.1–3.

Schröder, J., Müller Langer, F., Aakko Saksa, P., Winther, K., Baumgarten, W. and Lindgren, M., 2020. *Methanol as motor fuel – Summary report*. AMF Task 56 Report.

Kalwar, A., Singh, R.K., Gupta, A., Rajak, R., Gosakan, G. and Agarwal, A.K., 2023. ‘Combustion and performance evaluation of methanol fueled BS VI compliant light duty SI engine’. *ASME Open Journal of Engineering*, 2, article 041008. doi:10.1115/1.4063343.

Netzer, C., Seidel, L., Ravet, F. and Mauss, F., 2019. ‘Impact of surrogate formulation on 3D CFD engine knock prediction using detailed chemistry’. *Fuel*, 254, article 115626. doi:10.1016/ j.fuel.2019.115678.

Bradley, D., Morley, C., Gu, X.J. and Emerson, D.R., 2002. ‘Amplified pressure waves during autoignition: Relevance to CAI engines’. *SAE Technical Paper*, 2002-01-2868. doi:10.4271/2002-01-2868.

Keum, S. and Kuo, T.-W., 2019. ‘Damkohler number analysis on the effect of ozone on autoignition and flame propagation in internal combustion engines’. *Journal of Energy Resources Technology*, 141(11), article 112402. doi:10.1115/1.4043639.

Hayashi, S., Sakai, Y. and Tanaka, K., 2023. ‘A theoretical study on the relationship between pressure rise and the Damkohler number of end gas auto ignition in spark ignited engines’. *Combustion Theory and Modelling*, 27(4), pp.605–626. doi:10.1080/13647830.2023.2188259.

Rasaq, I., Al Attab, K.A., Enagi, I.I., Idroas, M.Y. and Mohamed, A.R., 2025. ‘Optimization of a cyclone combustor in flameless combustion using producer gas’. *Green Technology and Sustainability*, 3(2), pp.1–13. doi:10.1016/j.grets.2024.100154.

Otalvaro Marín, H.L. and Machuca Martínez, F., 2020. ‘Sizing of reactors by charts of Damkohler’s number for solutions of dimensionless design equations’. *Heliyon*, 6(11), article e05477. doi:10.1016/j.heliyon.2020.e05386.

Wijaya, W.Y., Shunsuke, K., Hirotatsu, W. and Ken, O., 2012. ‘Damkohler number as a descriptive parameter in methanol steam reforming and its integration with absorption heat pump system’. *Applied Energy*, 94, pp.141–147. doi:10.1016/j.apenergy.2012.01.041.

Attili, A., Bisetti, F., Mueller, M.E. and Pitsch, H., 2015. ‘Damkohler number effects on soot formation and growth in turbulent non premixed flames’. *Proceedings of the Combustion Institute*, 35(2), pp.1215–1223. doi:10.1016/j.proci.2014.05.084.

Wang, J., Tian, H., Zhang, R., Shen, B., Su, Y., Yu, H. and Zhang, Y., 2023. ‘Experimental investigation on the effects of direct injection timing on combustion, performance and emission characteristics of methanol/gasoline dual fuel DFSI engines under high load’. *Energies*, 16(24), article 47921. doi:10.3390/en16247921.

Stauch, R. and Maas U. 2008. ‘The ignition of methanol droplets in a laminar convective environment”, *Combustion and Flame*, 153 (1−2), pp. 45−57. doi:10.1016/j.combustflame.2007.09.002

Zhen, X., Wang, Y., Xu, S., Zhu, Y., Tao, C. and Xu, T., 2012. ‘The engine knock analysis – an overview’. *Applied Energy*, 92, pp.628–636. doi:10.1016/j.apenergy.2011.11.079.

Paltrinieri, S., Mortellaro, F., Silvestri, N., Medda, M., Corrigan, D. and Rolando, L., 2019. ‘Water injection contribution to enabling stoichiometric air to fuel ratio operation at rated power conditions of a high performance DISI single cylinder engine’. *SAE Technical Paper*, 2019-01-1148. doi:10.4271/2019-24-0173.

Bromberg, L. and Cheng, W., 2010. *Methanol as an alternative transportation fuel in the US: Options for sustainable and/or energy secure transportation*. Final Report. UT Battelle Subcontract No. 4000096701.

Wang, H., Ben, J., Zhang, S., Wang, K. and Xie, P. 2026. 'Green Methanol from CO2 Hydrogenation at Industrial Scale: Progress, Challenges, and Perspectives'. *Chem & Bio Engineering*. 3(2), pp. 159-178. doi: 10.1021/cbe.5c00113

Zhou, Y., Hong, W., Xie, F.-X., Li, X.-P., Su, Y. and Hu, Y.-B., 2022. ‘Potential of compression ratio and exhaust gas dilution for improving combustion and NO_x emission performance of methanol fueled PFI engines′. *Fuel*, 323, article 124321. doi:10.1016/j.fuel.2022.124197.

Yu, H., Su, Y., Shen, B., Zhang, Y., Wang, B. and Zhou, Y., 2024. ‘Effect of direct methanol injection based on low flow injectors on knock under heavy load gasoline engine operation’. *Fuel*, 357, article 130111. doi:10.1016/j.fuel.2023.129899.

Rehage, H. and Kind, M., 2020. ‘The first Damkohler number and its importance for characterizing the influence of mixing on competitive chemical reactions’. *Chemical Engineering Science*, 229, article 116007. doi:10.1016/j.ces.2020.116007.

Xu, C., Bao, Y., Li, X., Qian, L. and Oppong, F., 2023. ‘Pressure fluctuation and cellularization characteristics of 2-ethylfuran spherical expanding flames’. *Fuel*, 349, article 128627. doi:10.1016/j.fuel.2023.128627.

Geng, Z., Ding, C., Hu, J., Ampah, J.D., Jin, C. and Liu, H., 2025. ‘Stable inter solubility mechanisms of methanol–n heptane blends assisted by co solvents: Quantum chemical insights’. *Journal of Molecular Liquids*, 417, article 126626. doi:10.1016/j.molliq.2024.126626.

Li, S.-H., Wen, Z., Hou, J., Xi, S., Fang, P., Guo, X., Li, Y., Wang, Z. and Li, S., 2022. ‘Effects of ethanol and methanol on the combustion characteristics of gasoline using a revised variation disturbance method’. *ACS Omega*, 7(21), pp.17797–17810. doi:10.1021/acsomega.2c00991.

Methanol Institute, 2020. *Methanol: An emerging energy resource for the 21st century*. Policy Report.

Yates, A., Bell, A. and Swarts, A., 2010. ‘Insights relating to the autoignition characteristics of alcohol fuels’. *Fuel*, 89, pp.83–93. doi:10.1016/j.fuel.2009.06.037.

Wang, C.-M., Li, Y.-F., Xu, C.-S., Badawy, T., Sahu, A. and Jiang, C.-Z., 2019. ‘Methanol as an octane booster for gasoline fuels’. *Fuel*, 248, pp.76–84. doi:10.1016/j.fuel.2019.02.128.

Liu, Z., Zhang, Z., Rao, S. and Zheng, Z., 2024. ‘Study of water injection for suppressing knock in high compression ratio supercharged hybrid gasoline engines’. *Energy*, 287, article 129579. doi:10.1016/j.energy.2023.129702.

Wei, Y., Zhu, Z., Liu, S., Liu, H., Shi, Z. and Zeng, Z., 2023. ‘Injection strategy effects on mixture formation and combustion in heavy duty spark ignition methanol engines’. *Fuel*, 334, article 126688. doi:10.1016/j.fuel.2022.126680.

Duan, Q., Yin, X., Wang, X., Kou, H. and Zeng, K., 2022. ‘Knock combustion and direct injection effects in high compression ratio methanol engines’. *Fuel*, 311, article 122587. doi:10.1016/j.fuel.2021.122505.

Miganakallu, N., Yang, Z., Rogóż, R., Kapusta, Ł.J., Christensen, C., Barros, S. and Naber, J., 2020. ‘Effect of water–methanol blends on engine performance at borderline knock conditions in gasoline direct injection engines’. *Applied Energy*, 264, article 114750. doi:10.1016/j.apenergy.2020.114750.

Zhu, Z., Mu, Z., Wei, Y., Du, R., Guan, W. and Liu, S., 2022. ‘Cylinder to cylinder variation of knock and mixture formation effects in heavy duty spark ignition methanol engines’. *Energy*, 254, article 124235. doi:10.1016/j.energy.2022.124197.

Feng, H., Lai, K., Zheng, Z., Lin, S., Wu, X. and Tang, Q., 2024. ‘Effects of methanol direct injection and high compression ratio on the performance of spark ignition passenger car engines’. *Fuel*, 357, article 129901. doi:10.1016/j.fuel.2023.130052.

Shen, B., Su, Y., Yu, H., Zhang, Y., Lang, M. and Yang, H., 2023. ‘Experimental study on the effect of injection strategies on the combustion and emissions characteristics of a gasoline/methanol dual fuel turbocharged engine under high load’. *Energy*, 282, article 128870. doi:10.1016/j.energy.2023.128925.

Lee, B., Lee, H., Lim, D., Brigljević, B., Cho, W., Cho, H.-S., Kim, C.-H. and Lim, H., 2020. ‘Renewable methanol synthesis from renewable H_2 and captured CO_2: How can power to liquid technology be economically feasible?’. *Applied Energy*, 279, article 11582. doi:10.1016/j.apenergy. 2020.115827.

Methanol Institute, 2019. *Renewable methanol*. Washington, DC: Methanol Institute.

Deka, T.J., Osman, A.I., Baruah, D.C. and Rooney, D.W., 2022. 'Methanol fuel production, utilization, and techno economy: A review'. *Environmental Chemistry Letters*, 20(6), pp.3525–3554. doi:10.1007/s10311-022-01485-y.

Lyons, M., Durrant, P. and Kochhar, K., 2021. *Reaching zero with renewables: Capturing carbon*. Abu Dhabi: International Renewable Energy Agency, pp.1–108.

Cordero-Lanzac, T., Ramirez, A., Navajas, A., Gevers, L., Brunialti, S., Gandia, L.M., Aguayo, A.T., Sarathy, S.M. and Gascon, J., 2022. 'A techno economic and life cycle assessment for the production of green methanol from CO_2: Catalyst and process bottlenecks'. *Journal of Energy Chemistry*, 68, pp.255–266. doi:10.1016/j.jechem.2021.09.045.

Giuliano, A., Freda, C. and Catizzone, E., 2020. 'Techno economic assessment of bio syngas production for methanol synthesis: Focus on the water–gas shift and carbon capture sections'. *Bioengineering*, 7(3), article 70. doi:10.3390/bioengineering7030070.

Chen, Y., Li, H., Zhao, W., Zhang, W., Li, J., Li, W., Zheng, X., Yan, W., Zhang, W., Zhu, J., Si, R. and Zeng, J., 2019. 'Optimizing reaction paths for methanol synthesis from CO_2 hydrogenation via metal–ligand cooperativity'. *Nature Communications*, 10(1), article 1885. doi:10.1038/s41467-019-09918-z.

Ren, M., Zhang, Y., Wang, X. and Qiu, H., 2022. 'Catalytic hydrogenation of CO_2 to methanol: A review'. *Catalysts*, 12(4), article 403. doi:10.3390/catal12040403.

Liang, H., Zhang, G., Li, Z., Zhang, Y. and Fu, P., 2023. 'Catalytic hydrogenation of CO_2 to methanol over Cu based catalysts: Active site profiling and reaction pathway exploration'. *Fuel Processing Technology*, 252, article 107995. doi:10.1016/j.fuproc.2023.107995.

Zhu, J., Su, Y., Chai, J., Muravev, V., Kosinov, N. and Hensen, E.J.M., 2020. 'Mechanism and nature of active sites for methanol synthesis from CO/CO_2 on Cu/CeO_2'. *ACS Catalysis*, 10(19), pp.11532–11544. doi:10.1021/acscatal.0c02909.

Higham, M.D., Poh, Y.R., Catlow, C.R.A. and Krossing, I., 2025. 'Mechanism of CO_2 conversion to methanol on a highly representative Cu/ZnO interface'. *Journal of Catalysis*, 446, article 115997. doi:10.1016/j.jcat.2025.115997.

Ye, J., Dimitratos, N., Rossi, L.M., Thonemann, N., Beale, A.M. and Wojcieszak, R., 2025. 'Hydrogenation of CO_2 for sustainable fuel and chemical production'. *Science*, 387(6737), article adn9388. doi:10.1126/science.adn9388.

Kim, J., Yoo, Y., Kim, S., Beak, J., Oh, S.D., Lee, J. and Seo, M., 2024. 'Design and assessment of a mobile carbon capture system: Energy and exergy analyses'. *Energy Conversion and Management*, 300, article 117934. doi:10.1016/j.enconman.2023.117934.

Dziejarski, B., Krzyżynska, R. and Andersson, K., 2023. 'Current status of carbon capture, utilization, and storage technologies in the global economy: A technical assessment'. *Fuel*, 342, article 127776. doi:10.1016/j.fuel.2023.127776.

Wu, P.C. and Lin, C.Y., 2025. 'Feasibility and cost benefit analysis of methanol as a sustainable alternative fuel for ships'. *Journal of Marine Science and Engineering*, 13(5), article 973. doi:10.3390/jmse13050973.

Methanol Institute, 2023. *Marine methanol: Future proof shipping fuel*. Washington, DC: Methanol Institute, pp.1–3.

Shuangchen, M., Mengxuan, W., Tingting, H., Huihui, S., Bin, Z., Dongli, L. and Weizhong, C., 2013. 'Kinetic experimental study on desorption of decarbonization solution using the ammonia method'. *Chemical Engineering Journal*, 217, pp.22–27. doi:10.1016/j.cej.2012.11.098.

Zhang, M. and Guo, Y., 2014. 'A comprehensive model for regeneration of CO_2 capture using aqueous ammonia solutions'. *International Journal of Greenhouse Gas Control*, 29, pp.22–34. doi:10.1016/j.ijggc.2014.07.010.

Djettene, R., Dubois, L., Duprez, M.E., De Weireld, G. and Thomas, D., 2024. 'Integrated CO_2 capture and conversion to methanol: Techno economic and environmental assessment versus synthetic natural gas pathways'. *Journal of CO_2 Utilization*, 85, article 102879. doi:10.1016/ j.jcou.2024.102879.

Sajnani, S., Memon, M.A., Memon, S.A., Kumar, A., Mehvish, D., Mukarama, A.S., Zhou, W. and Liu, Y., 2025. 'CO_2 to methanol conversion: A bibliometric analysis with insights into reaction mechanisms and recent advances'. *Processes*, 13(2), article 314. doi:10.3390/pr13020314.

Nathrath, P., Kroll, F., Karmann, D., Geißelbrecht, M. and Schühle, P., 2025. 'Methanol production in a sustainable, mild, and competitive process: Concept launch and analysis'. *Green Chemistry*, 27(30), pp.9268–9279. doi:10.1039/D5GC01307K.

Li, S., Chen, R., Wang, J., Deng, S., Zhou, H., Fang, M., Zhang, H. and Yuan, X., 2024. 'Solar thermal assisted direct capture of CO_2 from ambient air for methanol synthesis'. *npj Materials Sustainability*, 2(1), article 14. doi:10.1038/S44296-024-00014-Y.

Hanson, E., Nwakile, C. and Hammed, V.O., 2025. 'Carbon capture, utilization, and storage (CCUS) technologies: Evaluating the effectiveness of advanced CCUS solutions for reducing CO_2 emissions'. *Results in Surfaces and Interfaces*, 18, article 100381. doi:10.1016/j.rsurfi.2024.100381.

Yang, N., Kang, F., Zhang, K., Zhou, Y. and Lin, W.-F., 2023. 'A strategy for CO_2 capture and utilization toward methanol production at industrial scale: An integrated high efficiency process based on multi criteria assessment'. *Energy Conversion and Management*, 293, article 117030. doi:10.1016/j.enconman.2023.117516.

Khojasteh Salkuyeh, Y., Ashrafi, O., Mostafavi, E. and Navarri, P., 2021. 'CO_2 utilization for methanol production – Part I: Process design and life cycle greenhouse gas assessment of alternative pathways'. *Journal of CO_2 Utilization*, 50, article 101608. doi:10.1016/j.jcou.2021.101608.

Battaglia, P., Buffo, G., Ferrero, D., Santarelli, M. and Lanzini, A., 2021. 'Methanol synthesis through CO_2 capture and hydrogenation: Thermal integration, energy performance, and techno economic assessment'. *Journal of CO_2 Utilization*, 44, article 101400. doi:10.1016/j.jcou.2020. 101407.

Ugwu, A., Osman, M., Zaabout, A. and Amini, S., 2022. 'Carbon capture, utilization, and storage in methanol production using dry reforming based chemical looping technology'. *Energy & Fuels*, 36, pp.9719–9735. doi:10.1021/acs.energyfuels.2c00620.

Ravikumar, D., Keoleian, G. and Miller, S., 2020. 'Environmental opportunity cost of using renewable energy for carbon capture and utilization in methanol production'. *Applied Energy*, 279, article 115835. doi:10.1016/j.apenergy.2020.115770.

Borisut, P. and Nuchitprasittichai, A., 2019. 'Methanol production via CO_2 hydrogenation: Sensitivity analysis and simulation based optimization'. *Frontiers in Energy Research*, 7, article 81. doi:10.3389/fenrg.2019.00081.

Herzog, H. and Vukmirovic, N., 1999. 'CO_2 sequestration: Opportunities and challenges'. Paper presented at the *Seventh Clean Coal Technology Conference*, Knoxville, TN.

Moghanloo, R.G., Yan, X., Law, G., Roshani, S., Babb, G. and Herron, W., 2017. 'Challenges associated with CO_2 sequestration and hydrocarbon recovery'. In: *Recent advances in carbon capture and storage*, pp.209 ff. doi:10.5772/67226.

Statista, 2020. *Share of CO_2 captured globally*. Statista Database.

Carlsson, I.Y., 2025. 'World's first commercial scale e methanol plant opens in Denmark'. *Reuters*, 7 August.

Carbon Recycling International (CRI), 2018. *Emission to liquid technology*. Carbon Recycling International.

Azarabadi, H. and Lackner, K.S., 2020. 'Post combustion capture versus direct air capture in decarbonizing US natural gas power'. *Environmental Science & Technology*, 54, pp.5102–5111. doi:10.1021/acs.est.0c00161.

Aghel, B., Janati, S., Wongwises, S. and Shadloo, M.S., 2022. 'Review of CO_2 capture using blended amine solutions'. *International Journal of Greenhouse Gas Control*, 119, article 103715. doi:10.1016/j.ijggc.2022.103715.

Asgharian, H., Marques, D.L., Iov, F., Liso, V., Nielsen, M.P., Thellufsen, J.Z., and Lund, H., 2024. 'Cryogenic carbon capture for future carbon neutral societies'. *International Journal of Greenhouse Gas Control*, 135, article 103867. doi:10.1016/j.ijggc.2024.104161.

Ketabchi, R.M., Babamohammadi, S., Davies, W.G., Gorbounov, M. and Soltani, S.M., 2023. 'Advances and challenges in carbon capture using bio based sorbents: A state of the art review'. *Carbon Capture Science & Technology*, 6, article 100087. doi:10.1016/j.ccst.2023.100087.

Li, G. and Yao, J., 2024. 'Direct air capture (DAC) for achieving net-zero CO_2 emissions: Advances, applications, and challenges'. *Eng*, 5(3), pp.1298–1336. doi:10.3390/eng5030069.

Gonzalez Olmos, R., Gutierrez Ortega, A., Sempere, J. and Nomen, R., 2022. 'Zeolite versus carbon adsorbents in carbon capture: Operational and life cycle comparison'. *Journal of CO_2 Utilization*, 55, pp.128–137. doi:10.1016/j.jcou.2021.101791.

Dai, Z. and Deng, L., 2024. 'Membrane technologies for CO_2 capture and separation: Progress toward industrial application'. *Separation and Purification Technology*, 335, article 123456. doi:10.1016/j.seppur.2023.126022.

Meng, L., Zheng, J., Yang, R., Peng, S., Sun, Y., Xie, J. and Li, D., 2023. 'Microseismic monitoring technologies and prospects for CCUS injection engineering'. *Energies*, 16, article 3101. doi:10.3390/en16073101.

Si, M. and Du, K., 2020. 'Development of a predictive emissions model using a gradient boosting machine learning method'. *Environmental Technology & Innovation*, 20, article 101028. doi:10.1016/j.eti.2020.101028.

Yeneneh, K. and Sufe, G., 2026. 'Experimental and ANN-based analysis of performance, combustion, and emission characteristics of a CI engine fueled with waste plastic oil-diethyl ether-diesel blends'. *PLoS One*, 21(2), article e0341627. doi:10.1371/journal.pone.0341627.

Guo, H., Başhan, V., Yu, C., Bolat, F., Demirel, H. and Tian, X., 2025. 'Effect of methanol injection timing on performance of marine diesel engines and emission reduction'. *Journal of Marine Science and Engineering*, 13(5), p.949. doi:10.3390/jmse13050949.

Wu, T., Yao, A., Yao, C., Pan, W., Wei, H., Chen, C. and Gao, J., 2018. 'Effects of diesel late injection on combustion and emissions of diesel/methanol dual fuel engines'. *Fuel*, 233, pp.317–327. doi:10.1016/j.fuel.2018.06.063.

Sequera, A.J., Parthasarathy, R.N. and Gollahalli, S.R., 2011. ‘Effects of fuel injection timing on biofuel combustion in diesel engines at partial load’. *Journal of Energy Resources Technology*, 133, article 022203. doi:10.1115/1.4003808.

Huang, G., Li, Z., Zhao, W., Zhang, Y., Li, J., He, Z., Qian, Y., Zhu, L. and Lu, X., 2020. ‘Influence of fuel injection strategies on combustion and emissions in intelligent charge compression ignition engines fueled with methanol and biodiesel’. *Fuel*, 274, article 117851. doi:10.1016/j.fuel.2020.117851.

Yin, X., Yan, Y., Ren, X., Yu, L., Duan, H., Hu, E. and Zeng, K., 2025. ‘Effects of methanol energy substitution ratio and diesel injection timing in methanol/diesel dual fuel direct injection engines’. *Fuel*, 382(B), article 133773. doi:10.1016/j.fuel.2024.133773.

Kumar, D., Sonawane, U., Chandra, K. and Agarwal, A.K., 2022. ‘Experimental investigation of methanol fumigation via port fuel injection in preheated intake air of a single cylinder dual fuel diesel engine’. *Fuel*, 324, article 124340. doi:10.1016/j.fuel.2022.124340.

El Seesy, A.I., Waly, M.S., Alhassan Nasser, N.A. and El Zoheiry, R.M., 2022. ‘Improvement of combustion, emission, and stability characteristics of diesel–methanol blends using n decanol as a co solvent’. *Scientific Reports*, 12, article 20326. doi:10.1038/s41598-022-20326-0.

Li, Z., Wang, Y., Wang, Y., Yin, Z., Gao, Z., Ye, Z. and Zhen, X., 2022. ‘Effects of fuel injection timing and methanol split ratio in M/D/M strategies for diesel/methanol dual fuel direct injection engines’. *Fuel*, 325, article 124970. doi:10.1016/j.fuel.2022.124970.

Vargün, M., Yılmaz, I.T., Özsezen, A.N. and Sayın, C., 2025. ‘Combustion parameters and exhaust characteristics of diesel engines using alternative fuels at different start of injection and gas pilot proportions’. *Processes*, 13, article 3024. doi:10.3390/pr13093024.

Svensson, E., Tunér, M. and Verhelst, S., 2019. ‘Influence of injection strategies on engine efficiency in methanol partially premixed combustion engines’. *SAE International Journal of Advances and Current Practices in Mobility*, 2(2), pp.653–671. doi:10.4271/2019-24-0116.

Treacy, M., Xu, L., Fatehi, H., Kaario, O. and Bai, X.S., 2024. ‘Performance of a methanol fueled direct injection compression ignition heavy duty engine under low temperature combustion conditions’. *Energies*, 17(17), article 4307. doi:10.3390/en17174307.